



HAL
open science

Impairment-aware design and performance evaluation of all-optical wavelength convertible networks

Hussein Chouman

► **To cite this version:**

Hussein Chouman. Impairment-aware design and performance evaluation of all-optical wavelength convertible networks. Networking and Internet Architecture [cs.NI]. Université Paris Saclay (COMUE), 2019. English. NNT: 2019SACLT011 . tel-02127935

HAL Id: tel-02127935

<https://pastel.hal.science/tel-02127935>

Submitted on 13 May 2019

HAL is a multi-disciplinary open access archive for the deposit and dissemination of scientific research documents, whether they are published or not. The documents may come from teaching and research institutions in France or abroad, or from public or private research centers.

L'archive ouverte pluridisciplinaire **HAL**, est destinée au dépôt et à la diffusion de documents scientifiques de niveau recherche, publiés ou non, émanant des établissements d'enseignement et de recherche français ou étrangers, des laboratoires publics ou privés.

Impairment-aware design and performance evaluation of all-optical wavelength convertible networks

Thèse de doctorat de l'Université Paris-Saclay
préparée à Télécom-ParisTech

École doctorale n° 580 "Sciences et Technologies de
l'Information et de la Communication" (STIC)
Spécialité de doctorat: Réseaux, Information, Communications

Thèse présentée et soutenue à Télécom-ParisTech Paris, le 22 Mars 2019, par

Hussein Chouman

Composition du jury:

Bernard COUSIN Professeur, Université de Rennes 1, IRISA	Rapporteur
Idelfonso TAFUR MONROY Professeur, Eindhoven University of Technology	Rapporteur
Christine TREMBLAY Professeur, École de technologie supérieure	Examinatrice
Philippe GRAVEY Directeur d'études, IMT Atlantique	Examineur
Hind CASTEL Professeur, Télécom SudParis	Examinatrice
Catherine LEPERS Professeur, Télécom SudParis	Invité
Dominique CHIARONI Ingénieur de Recherche, Nokia Bell Labs France	Invité
Cédric WARE Maître de Conférences-HDR, Télécom ParisTech	Directeur de thèse
Mounia LOURDIANE Maître de Conférences, Télécom SudParis	Encadrant de thèse



To the loving memory of my father Hasan Chouman.

To my mother Salwa Chouman



Acknowledgments

Contents

Acknowledgments	iii
Table of contents	iv
List of Figures	vi
List of Tables	viii
List of Abbreviations	ix
1 Introduction	1
1.1 Optical Networks Evolution	1
1.1.1 Towards All-Optical Networks	1
1.1.2 Optical Networks Capacity Improvement	2
1.2 Motivation and Objective	4
1.3 Thesis Structure	5
2 Wavelength Convertible Networks Design	7
2.1 Introduction	7
2.2 RWA in Wavelength Continuous Network	8
2.2.1 Optimization Approaches	8
2.2.2 Decoupling RWA	9
2.2.3 PLI-RWA	13
2.3 Wavelength Converters in Optical Networks	14
2.3.1 Wavelength Conversion Benefits	14
2.3.2 How to Benefit From Wavelength Converters In Optical Networks	17
2.4 Conclusion	22
3 Transmission Layer Model	23
3.1 Introduction	23
3.2 Transmission Impairments	24
3.2.1 Linear impairments	24
3.2.2 Non-linear Impairments	25
3.3 Compensated Transmission	27
3.3.1 MLR Model	28

3.3.2	System Performance	31
3.4	Uncompensated Transmission Model	32
3.4.1	GN-model	33
3.4.2	IGN-model	35
3.4.3	System Performance	36
3.5	Conclusion	39
4	Simulation Results: Offline Traffic assumption	41
4.1	Introduction	41
4.2	Network Model	43
4.2.1	Simulation Parameters	44
4.2.2	Performance Parameters	46
4.3	Simulation Results	47
4.3.1	Sensitivity Of The Gain Of Using Wavelength Converters to TSO	48
4.3.2	TD vs DI in Wavelength Continuous and Wavelength Convertible Networks	49
4.4	Conclusion	52
5	Simulation Results: Online Traffic assumption	55
5.1	Introduction	55
5.2	Routing, Modulation Format and Wavelength Allocation Algorithms . . .	56
5.2.1	Heuristic algorithm	56
5.2.2	Heuristics Flavors	58
5.2.3	Simulation Parameters	58
5.2.4	Performance Metrics	60
5.3	Simulation Results: The Gain of Using OEO-WCs	61
5.3.1	Sensitivity to the Number of Alternative Paths	62
5.3.2	Sensitivity to Wavelength Assignment Algorithms	63
5.3.3	Sensitivity to Routing algorithms	65
5.4	Simulation Results: Network Gain from Using AO-WCs	68
5.5	Conclusion	72
6	Conclusions and future work	73
6.1	Summary and Conclusions	73
6.2	Future Research Proposals	75
	Bibliography	77

List of Figures

1.1	Bit-rates Evolution [1]	5
2.1	Various PLI-RWA approaches [2]	12
2.2	Example about fragmentation problem and the role of a wavelength converter in a network	14
2.3	Node with complete wavelength conversion [3]	15
2.4	Node with partial wavelength conversion [3]	15
2.5	Example H-hop network with a single traffic stream using all the links [4]	17
2.6	25-node mesh torus network topology	19
3.1	Point-to-point link schematic	27
3.2	BER vs P_{ch} for different number of spans	31
3.3	BER vs P_{ch} for different number of channels	32
3.4	Maximum number of spans reached by each modulation format versus P_{ch} at BER= 10^{-3}	33
3.5	Point-to-point link schematic	37
3.6	OSNR vs P_{ch} for different N_s	38
3.7	OSNR vs P_{ch} for different N_{ch}	39
4.1	Heuristic skeleton	42
4.2	Different candidates of the heuristic used.	43
4.3	17-Node German network topology.	45
4.4	BTP vs. ATD using TD-based heuristics.	47
4.5	BTP vs. ATD using DI-based heuristics.	47
4.6	FUP vs. ATD using different heuristic candidate.	48
4.7	No. lihtpaths using 16-QAM vs. ATD using different heuristic candidates.	50
4.8	No. lihtpaths using PM-QPSK vs. ATD using different heuristic candidates.	50
4.9	BTP vs. ATD for TD vs DI in wavelength-continuous networks.	51
4.10	BTP vs. ATD for TD vs DI in wavelength-convertible networks.	51
5.1	Discrete events: arrival and departures.	56
5.2	Different flavors of the heuristic used.	59
5.3	Blocking versus arrival rate (Λ) using FAR-FF _{NWC} and FAR-FF _{OEO} heuristics at different κ	61

5.4	Blocking versus arrival rate (Λ) using LLR-FF _{NWC} and LLR-FF _{OEO} heuristics at different κ .	62
5.5	Blocking versus arrival rate (Λ) using FAR-FF _{OEO} and FAR-MC _{OEO} heuristics at different κ .	62
5.6	Blocking versus arrival rate (Λ) using LLR-FF _{OEO} and LLR-MC _{OEO} heuristics at different κ .	63
5.7	Number of conversions vs. arrival rate using FAR-FF _{OEO} and FAR-MC _{OEO} heuristics at different κ .	64
5.8	Number of conversions vs. arrival rate using LLR-FF _{OEO} and LLR-MC _{OEO} heuristics at different κ .	64
5.9	Blocking versus arrival rate (Λ) using FAR-FF _{OEO} and LLR-FF _{OEO} heuristics at different κ .	66
5.10	Blocking versus arrival rate (Λ) using FAR-MC _{OEO} and LLR-MC _{OEO} heuristics at different κ .	66
5.11	% lightpaths using 200 Gb/s vs. Λ in FAR-FF _{OEO} and LLR-FF _{OEO} heuristics at different κ .	67
5.12	% lightpaths using 200 Gb/s vs. Λ in FAR-MC _{OEO} and LLR-MC _{OEO} heuristics at different κ .	67
5.13	% Blocking vs. C at $\Lambda=95$, R= 2x50 GHz and $\kappa=6$.	68
5.14	% Blocking vs. C at $\Lambda=95$, R= 4x50 GHz and $\kappa=6$.	69
5.15	$Gain_{relative}$ vs. C at $\Lambda=95$, R= 4x50 GHz and $\kappa=6$.	69
5.16	Number of conversions vs. C at $\Lambda=95$, R= 4x50 GHz and $\kappa=6$ using FAR.	71
5.17	Number of conversions vs. C at $\Lambda=95$, R= 4x50 GHz and $\kappa=6$ using LLR.	71

List of Tables

3.1	The characteristics of fiber used [5]	28
-----	---	----

List of Abbreviations

AO-WC	all-optical wavelength converter
ATD	average traffic per demand
BER	bit-error-rate
BTP	percentage of blocked traffic
CAPEX	capital expenditure
CD	chromatic dispersion
DCF	dispersion compensating fiber
DQPSK	differential quadrature phase-shift keying
EDFA	erbium-doped-fiber amplifier
FAR	fixed-alternative routing FEC
FF	first-fit wavelength assignment algorithm
FUP	fiber utilized percentage
FWM	four-wave mixing
GN	Gaussian-noise
ILP	integer linear programming
LLR	least-loaded routing
MC	minimum number of conversion wavelength assignment algorithm
MLR	mixed line rate
NLI	non-linear-interference
OEO	optical-to-electrical-to-optical
OOK	on-off keying
OPEX	operational expense or the operational expenditure
OSNR	optical-signal-to-noise ratio
PM-QPSK	polarization-multiplexed quadrature phase-shift keying
PMD	polarization mode dispersion
PSD	power-spectral-density

QAM	quadrature amplitude modulation
QoT	quality of transmission
RWA	routing and wavelength allocation
SMF	single-mode fiber
SPM	self-phase modulation
TSO	traffic serving ordering
UT	uncompensated transmission
WCC	wavelength continuity constraint
WDM	wavelength-division multiplexing
WLCR	weighted-least-congested-route
XPM	cross-phase modulation

Chapter 1

Introduction

1.1 Optical Networks Evolution

1.1.1 Towards All-Optical Networks

Optical networks have played a critical role in making possible the global communication revolution that has brought the world together, enabled emerging countries to join the digital world economy and improved the quality of life for people all around the globe. They are considered the cornerstone of future Internet especially with emerging applications such as Internet Protocol Television (IPTV), video on demand, cloud computing and grid computing applications. Moreover, they provide the physical infrastructure of the core and metro backbone networks, which makes it a need to increase optical network capacity while existing services for the end-user have to get cheaper and cheaper.

The history of modern day fiber optic communication dates back to 1960s when Dr. Charles K. Kao proposed that the losses in an optical fiber based on silica glass can be reduced to 20 dB/km by removal of contaminants. Since the late 1980s, fiber-optic networks have steadily become the bedrock for the ever-expanding global telecommunications system. Early fiber-optic links, such as the eighth transatlantic telecommunications cable installed in 1988, were relatively simple systems by today's standards and used on-off keying (OOK) to transmit a few hundred megabits per second over a single optical fiber where data were impressed on a single optical channel [6]. The optical signal, because of fiber loss and possible signal distortion, was detected and electrically regenerated and then converted back to optical at all intermediates nodes along the path from source node to destination node, this is called optical-to-electrical-to-optical (OEO) regeneration, it is know as the opaque mode of the network [7, 8]. As a result of OEO, the opaque mode has the advantage of traffic grooming which enables using efficiently the optical channel capacity where we can groom small demands together if the chan-

nels are not already occupied. Moreover, signal regeneration is essential to re-amplify, re-shape and re-time optical signal (it's know to be 3R) to improve signal quality and allow it to reach long distance. Nevertheless, we can't ignore the fact that the signal's regeneration cost increases as the rate of the signal and the modulation format complexity increases. Thus, it significantly impact the capital expenditure (CAPEX) and the operational expense or the operational expenditure (OPEX).

By the early 1990s, wavelength-division-multiplexing (WDM) has been realized in optical transmission where data channel is modulated onto optical carrier with a unique wavelength then, optical carriers are multiplexed and transmitted in a single fiber. However, OEO regeneration represented an obstacle for commercial viability of WDM transmission system before the advent of optical amplifiers due to the high cost of signal regeneration for N wavelengths which makes the implementation cost to upgrade the system increase roughly proportion to the capacity increase [6]. Therefore, the availability of optical amplifiers, especially the most successful one erbium-doped-fiber amplifier (EDFA), and the fact that a single amplifier can simultaneously amplify multiple wavelengths, enable WDM being economically possible.

The other technology that underpinned the optical networks is the optical switching which enabled the switching from one of n input fiber routes to any of n output fiber routes and does so for all the wavelengths carried by the fiber. Thus, the signal is kept in the optical domain without any OEO regeneration in the middle, neither for signal amplification nor for switching, hence, it decreases the CAPEX and OPEX. This represents the second mode of the network called the all-optical network or transparent network [7]. The third mode of the network is the the translucent mode which is a compromise between the opaque mode and the all-optical transparent one. It takes benefit from both of them in such a way that the best trade-off between traffic grooming, and signal regeneration is found, optimizing cost. Hence, every node can be opaque, transparent or both according to the traffic to satisfy, routing constraints, regenerator placement strategy, and optimization objective [8].

1.1.2 Optical Networks Capacity Improvement

Due to the continuous growth of traffic and since the EDFA-based intensity modulation with direct-detection were reaching their limits in serving the network traffic demands, and in order to sustain such traffic increase, while existing services for end-users have to get cheaper and cheaper, there were different approaches by the operators to increase the network's capacity. The simplest solution is to install new fiber whenever there is a bandwidth need which will result in a need to install new amplifiers and WDM system deployment. Thus, it is not an economical solution which usually kept as a last resort [8]. The second approach is based on increasing the number of WDM channels in the C-band by reducing the channel spacing between the channels. The two main examples

are Dense Wavelength Division Multiplexing (DWDM) and Ultra Dense Wavelength Division Multiplexing (UDWDM) technologies. On the one hand, DWDM technology uses a 0.4 nm (50 GHz) channel spacing which results in more than 80 channels per fiber in the EDFA amplifier C-Band, is showing a very good performance in terms of reach. On the other hand, the studies performed on an Ultra Dense Wavelength Division Multiplexing (UDWDM) technology with even narrower spacing (< 0.2 nm) and smaller per-channel signal bandwidth. However, it does not match higher data-rates' (e.g., 100 Gb/s and beyond) channel spacing requirement which needs more than 25 GHz [8].

As a result to the constraints on the bandwidth imposed by optical amplifiers and ultimately by the fiber itself, it is important to maximize spectral efficiency, measured in bit/s/Hz to increase the fiber capacity [9]. Therefore, coherent technologies, which have restarted to attract a large interest [10] by the year 2005, made it possible to have higher spectral-efficient multi-level modulation formats such as M-ary phase shift keying and quadrature amplitude modulation (QAM). Consequently, the per-channel data-rate is increased using high-level modulation formats [9]. Therefore, it allowed a breakthrough in fiber's capacity evolution offering enough capacity for the observed exponential growth of traffic. Nevertheless, the larger the number of constellation points is, the more sensitive to impairments the transmission is, which can involve significant impact on the transmission reach [8]. Thus, based on the availability of different bit-rates, and the trade-off between the transmission reach and the channel's rate, we have three categories for optical network. In the first category, the highest single rate is used without considering the traffic demand volume, this is called the single-line-rate (SLR). In the second category, networks mix optical transponders with different fixed data-rates, which can have different optical reaches, it is known as mixed-line-rate (MLR) which allows overcoming the over-design challenges of SLR transponders. The third category concerns elastic transponders with on-demand data-rate adaptation [11, 12].

The ability to have higher-order modulation format based on coherent detection has increased fiber's capacity, however, increasing the channel bit-rate beyond beyond 100 Gb/s at the same optical reach is increasingly difficult due to the nonlinear Shannon limit and increasing the baud-rate considerably is also difficult [13]. Moreover, the need to decrease the cost per bit and energy per bit by increasing spectral efficiency is very critical. Additionally, since capacity limit of optical fiber should be reached soon, there is a renewed interest on spectrum utilization. Indeed, the conventional fixed-grid optical networks are characterized by a non-optimized use of spectrum resources as a fixed channel spacing must be used, even if the required signal spectrum amount is smaller. Modern photonic integrated circuits technology have led to a change in the optical network architecture from rigid and homogeneous to flexible and heterogeneous in terms of the bit-rate, center frequency spacing, modulation format, and optical reach. The elastic optical network is a network architecture towards beyond the 100 Gb/s era [13].

1.2 Motivation and Objective

According to Cisco [14], the overall IP traffic is exponentially growing and will follow the same trend in the coming years. Thus, the major lines rates in metro/core network are 100 Gb/s and beyond [1, 13]. Additionally, due to the need to enhance the flexibility and reconfigurability in the network that is moving toward software-defined-network and consequently, instead of using separate transceiver for each modulation format, elastic transponders based on multi-level modulation formats are able to switch among different modulation formats [15, 16]. However, due to the need to have all-optical networks in order to reduce the OEO-conversions, we can't ignore the trade-off between the transmission reach and channel's rate which leads to a very low transmission reach for the highest-order modulation formats. Another constraint resulting from transparent optical networks is the need of optical channels to conserve the same wavelength in all the fibers between the source and destination node (wavelength continuity constraint (WCC) is explained in details in Sec. 2.3.1). This problem results in non-efficient use of wavelength resources and blocking some demands which is solved by using wavelength converters.

The only commercially available products that offer wavelength conversion are OEO-regenerators (in this dissertation, we will refer to them by OEO-WCs). However, they suffer from the fact that their cost increases as the data-rate increases [17]. Thus, using them only for wavelength conversion functionality (in case a regeneration is not required) is a costly solution. Hence, all-optical wavelength converters (AO-WCs), which shift signals' wavelengths in the optical domain, become a crucial need to avoid the use of regenerators in transparent networks. Demonstrated AO-WCs in laboratories [18–27] have some limitations compared to OEO-WCs: the channel's quality of transmission (QoT) is slightly degraded after every conversion, thus, the more the channel undergoes conversion, the more its QoT is worsened. Moreover, it is not possible to convert from any wavelength to any wavelength (detailed in Sec.2.3.1.1) as in OEO-WCs case [27, 28]. Therefore, these limitation might affect wavelength converters contributions in optical networks which depend on a lot of factors as detailed in Ch. 2 [4].

Thus, using AO-WCs will add some design constraints which should be taken into consideration to optimize their contribution. In literature, there are few works that consider AO-WCs' limitations at the network level [22–24]. They show that these limitations aren't an obstacle to obtain the same network blocking performance compared to the case of using OEO-WCs, which don't have any limitations. However, this need to be deeply investigated considering all the factors mentioned above and see which one optimizing the contribution of AO-WCs in optical networks. Therefore, in this thesis work,

- We will design transparent optical networks, based on WDM of the fixed-grid or the conventional channel spacing of 50 GHz, assuming the online and the offline

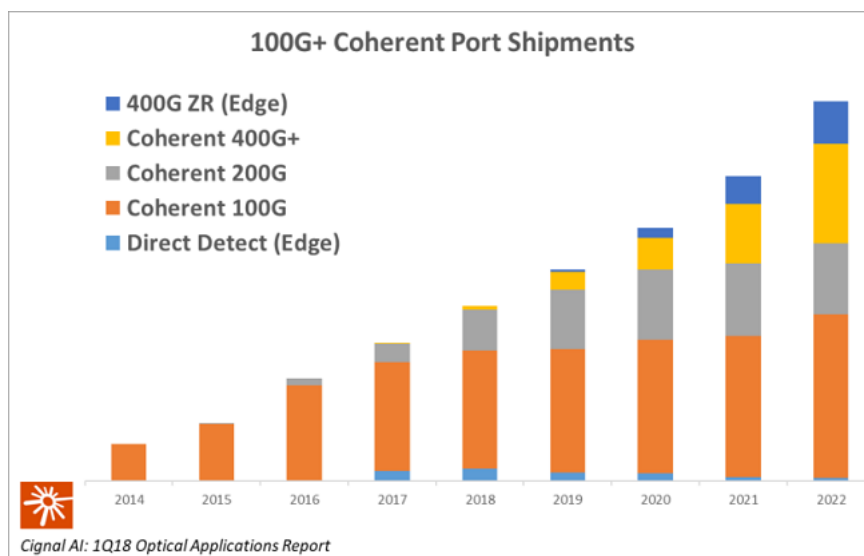


Figure 1.1: Bit-rates Evolution [1]

traffic assumptions.

- we will study if AO-WCs with their limitations can give the same performance enhancement as OEO-WCs in multi-rate transparent optical networks.
- We will consider two different transmission layers, the MLR and the elastic transponder. The reasons of using two different modulation formats categories is that during the start of the thesis, there was an interest in the MLR where the operators were upgrading the network containing the legacy 10 Gb/s OOK by adding 100 Gb/s PM-QPSK. However, due to the traffic growth and since the major lines in metro and core network are 100 Gb/s and beyond [13] as shown in Fig 1.1 which displays bit-rates evolution by Cisco, we moved in the second part of this thesis to the elastic transponders that enable us to vary the modulation format toward the 400 Gb/s 64-QAM.

1.3 Thesis Structure

This dissertation covers the following topics:

- This chapter provides a background for the proposed research, the motivation and the overall objectives.
- In Ch. 2, we will show a brief survey on:

1. An overview about optical networks design problems and different approaches to solve them.
 2. A survey on the work done in literature regarding AO-WCs and how to benefit from wavelength converter in a optical networks.
- In Ch. 3, we will present the optical transmission impairments in optical communications. Afterwards, we will introduce the transmission layer models used to estimate the QoT performance in two different scenarios based on different bit-rates and modulation formats used:
 1. The dispersion-compensated transmission using MLR 10 Gb/s OOK based on direct detection and 100 Gb/s PM-QPSK based on coherent detection case. QoT estimation in this case be based on the Gaussian approximation. Moreover, we will show the experimental results hold in ETS laboratories, in Montréal, in the MLR scenario.
 2. The dispersion-uncompensated transmission using only coherent-detection based modulation formats in which the QoT estimation is done using the Gaussian-noise (GN) model.
 - In Ch. 4, we will study the dependence of wavelength converters contributions on the traffic serving order (TSO) of the demands of the traffic matrix based on the LogNormal distribution. Therefore, the chapter will start by showing the heuristics used (the routing algorithm, the wavelength assignment algorithm and the modulation format allocation algorithms) and we will define the TSOs used. Finally, we will show the simulation results and conclusion.
 - In Ch. 5, we will study the performance of optical networks using AO-WCs and compare the results to the case when OEO-WCs are used in order to find the optimum conditions of AO-WCs to give contributions as OEO-WCs. Therefore, the chapter will start by showing the heuristics used (the routing algorithms, the wavelength assignment algorithms and the modulation format allocation algorithm). Finally, we will show the simulation results and conclusion.
 - Finally, Ch. 6 draws the conclusions, and includes some suggestions for possible future research plans.

Chapter 2

Wavelength Convertible Networks Design

2.1 Introduction

In WDM transparent optical networks, a traffic demand is sent from a source node s to a destination node d using a wavelength channel called a lightpath, which is a connection in the optical layer similar to the one in a circuit-switched network. To establish a lightpath, a route has to be chosen and a particular wavelength has to be assigned to it. This problem is known as the *routing and wavelength assignment problem* (RWA).

Solving the RWA problem in transparent networks is subject to the following constraints. Firstly, if wavelength conversion capability is not available at intermediate nodes, the same wavelength must be assigned along the entire route over different links traversed by the lightpath; this is called the WCC (in this dissertation, we will refer to the cases where converters are not used as *wavelength continuous networks*). Secondly, lightpaths that are traversing a common physical link cannot be assigned the same wavelength. This is called the wavelength clash constraint. Thirdly, physical layer impairments accumulation affects the signal transmission reach and it is considered as additional constraints for the RWA decisions which is known as physical layer impairment aware (PLI-RWA) or QoT-aware RWA (QoT-RWA). On the other hand, if wavelength conversion is enabled (in this dissertation, we will refer to the cases where converters are used as *wavelength convertible networks*), the WCC is released and thus, it improves network blocking performance and link utilization (defined in Sec. 2.3.1). However, this enhancement is not straightforward and it is subject to many conditions that will be detailed afterward.

Therefore, this chapter is organized as follows. Sec. 2.2 presents a literature survey

about the basic fundamentals of optical networks design and the possible approaches to solve RWA problem. Sec. 2.3 presents a brief summary about types of wavelength converters and their required characteristics at the network level. Afterwards, the conditions or the scenarios that optimize the gain from wavelength-converters are detailed. Finally, Sec.2.4 concludes this chapter and perspective work.

2.2 RWA in Wavelength Continuous Network

Traffic demands are typically assumed to be either static (demands are known beforehand) or dynamic (demands arrive unexpectedly with random holding times). RWA for the static assumption is also known as the network planning phase, which typically occurs before a network is deployed, consists of processing a large set of demands (traffic matrix) at one time. Therefore, the main emphasis of network planning is on accommodating the traffic matrix and minimizing the resources needed, such as number of wavelengths, fibers or number of transceivers in a network; alternatively, it aims to allocate the highest number of lightpaths, e.g. minimize the blocking, for a given number of wavelengths and a traffic matrix. On the other hand, for the dynamic traffic assumption, demands are generally processed sequentially. It is known as the network operation phase and it aims to set up lightpaths and assign wavelengths in a manner which minimizes the blocking or maximizes the number of connections in the network at any time taking into consideration that requests need to be processed online and thus, the solution must be computationally simple. Therefore, in this section we will introduce different approaches that have been suggested in literature to handle the RWA problem.

2.2.1 Optimization Approaches

Integer linear programming formulation

A linear program is a mathematical model, that aims to find a set of non-negative values for variables, which maximizes or minimizes a linear objective function while satisfying a system of linear constraints. A linear program, in which all variables are required to be integers, is called an integer linear program (ILP). If just some of variables are integers, the ILP is called mixed-ILP [29]. The static RWA is formulated as mixed-ILP problem and it has been shown that it is NP-complete (non-deterministic polynomial time) [30], which means that the time required, using any currently known algorithms, to find an optimal solution for such problems increases exponentially as the size of the problem increases. Therefore, polynomial-time algorithms or heuristics which result in sub-optimal solutions are preferred [29].

Heuristics

For real-sized networks, because of the high complexity of the problem doesn't

allow to find the optimal solution in reasonable time, one often has to use a heuristic algorithm. A heuristic approach is the one in which the algorithm goes in a deterministic way following a set of instructions; it works reasonably well in many cases, but for which there is no proof that it will always produce an optimal result. On the other hand, this approach is very fast and easy to implement. An example of heuristics algorithms is the greedy algorithm which is any algorithm that follows the problem solving of making the locally optimum choice at each stage with the hope of finding the global optimum. Greedy algorithms usually use an iterative process until a certain condition is reached for example, authors in [31, 32] served the demands of the traffic matrix iteratively, for that purpose, they have suggested different traffic serving orderings based either on the traffic demands' volume (connection demands ordered according to their requested bit-rate, and serve first the demand that requires the highest bit-rate) or based on the the demands' shortest-path (connection demands ordered according to the physical length of their shortest-path, and serve first the demand whose shortest-path utilizes the lowest physical route length). The performance metric used are the percentage of the blocked demands and the network utilization or fiber occupancy.

Meta-heuristics

A meta-heuristic is a heuristic method to solve a general class of computational problems in the hope of obtaining a more efficient or more robust procedure. It designates a computational method that optimizes a problem by iteratively trying to improve a candidate solution with regard to a given performance metric. Meta-heuristics make few or no assumptions about the problem being optimized and can search very large spaces of candidate solutions. However, they do not guarantee an optimal solution is ever found. There are many meta-heuristic algorithms, among which genetic algorithm, tabu-search and simulated-annealing are the most popular and widely applied to solve network optimization problems [29].

2.2.2 Decoupling RWA

Solving routing and wavelength assignment together is hard, thus, the problem is usually decoupled in two sub-problems, so-called routing problem and wavelength assignment problem, and solved sequentially. Usually, the routing sub-problem is solved first and then the wavelength assignment is carried out for the selected route. In this section, we will do a brief review about solutions offered in the literature for each sub-problem [29, 30, 33].

2.2.2.1 Routing sub-problem

In this section, we focus on various approaches proposed in literature to solve the routing sub-problem [33]:

ILP formulation for static lightpath establishment

Similar to RWA, the routing problem can also be formulated as an ILP ; the primary difference between this formulation and the RWA formulation is that WCC is not imposed. Instead, WCC is imposed when actually assigning wavelengths to the lightpaths.

Fixed Routing

This approach always chooses the same fixed route, for instance, the shortest-path-routing calculated using Dijkstra's algorithm [34], or any predetermined path. The connection is blocked in the case of failure of any link in the route or the non-availability of a common wavelength in the path. This is a straightforward approach, however it can't handle a failure in the network and leads to higher blocking, thus, the routing scheme must either consider alternate paths or dynamically fixed route.

Fixed-Alternative Routing (FAR)

This algorithm considers multiple routes between s and d of the traffic demand, This set of routes is called alternate-routes; it could be the first, second, ..., and k^{th} shortest paths. Moreover, alternate-routes could be link-disjoint routes (don't have any common link with the first route) in some cases. Therefore, among these routes, fixed-alternate routing, unlike fixed-routing, tries to establish connection on the first available route; thus, it improves network blocking performance and provides some degree of fault tolerance upon link failure. On the other hand, unlike adaptive routing, it doesn't consider the network state which may lead to the congestion of the network.

Adaptive Routing

In this algorithm, the route from s to d is chosen dynamically based on the network state. For instance, the least-loaded routing (LLR) algorithm routes the connection on the path with the lowest congestion, which is measured based on the number of wavelengths available on the link, among the predetermined routes. The performance of LLR showed that it is better than that of the *fixed-alternate* routing, however, it has a higher complexity [29].

The routing algorithms used in this thesis are the FAR and the LLR algorithms due to their importance as will be shown in Sec. 2.3.2.

2.2.2.2 Wavelength Assignment Sub-problem

In this section, we first introduce the static wavelength-assignment problem, i.e., given a set of lightpaths and their routes, assign a wavelength to each lightpath. One approach to solving this problem is to formulate it as a graph-coloring. Afterwards, we discuss different wavelength-assignment heuristics proposed in literature [30]:

Static wavelength assignment

Static wavelength assignment aims to assign wavelengths to different lightpaths in a manner which minimizes the number of wavelengths used under the WCC and thus, it reduces to the graph coloring problem as stated below:

1. Construct an auxiliary graph $G(V, E)$ such that each lightpath in the system is represented as a node in an auxiliary graph G .
2. There is an un-directed edge between two nodes in a graph G if the corresponding lightpaths pass through a common physical fiber link.
3. The nodes of the graph are colored such that no two adjacent nodes have the same color.

This problem has been shown to be NP-complete, therefore heuristics algorithms are used to find sub-optimal solutions.

Random

This scheme chooses a wavelength randomly (usually with uniform distribution) among the set of available wavelengths on the required route.

First-fit (FF)

In this scheme, all wavelengths are numbered. While searching for an available wavelength, a lower-numbered wavelength is considered before the higher-numbered one and thus, the first available wavelength is selected. The idea behind this scheme is to pack all the in-use wavelengths toward the lower end of the wavelength space so that continuous longer paths towards the higher end of the wavelength space will have a higher probability of being available. This algorithm performs well in terms of blocking probability and fairness, and is preferred in practice because of its low computational complexity.

Least-used

This scheme chooses the wavelength that is least used in the network in an attempt to balance the load among all wavelengths. This scheme also requires additional storage and computation cost (global information is required to compute the least-used wavelength); thus, it is not preferred in practice.

Most-used

If instead of using the least-used wavelength, we allocate a connection to the most-used wavelength, we implement the *Most-used* wavelength assignment algorithm.

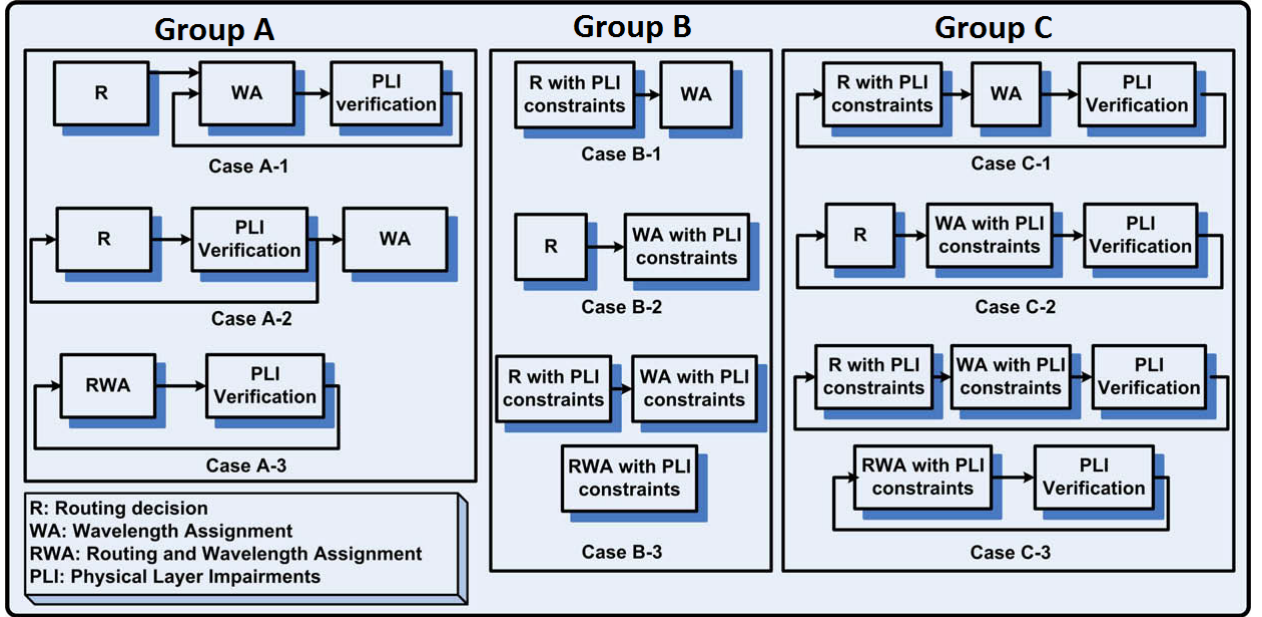


Figure 2.1: Various PLI-RWA approaches [2]

Most-used algorithms slightly outperforms the FF algorithm, however, it is not preferred since it requires additional storage and computational cost similar to those in Least-used algorithm.

Max-sum

Max-sum attempts to minimize network blocking by maximizing the remaining path capacities after lightpath establishment. This scheme was proposed for multi-fiber networks, but it can also be applied to single-fiber network.

Least-loaded

This scheme was proposed for multi-fiber networks. It selects the wavelength that has the largest residual capacity on the most-loaded link along route. For example, if each link has $m = 5$ fibers where each fiber has only two wavelengths λ_i and λ_j , thus, $m_i = 5$ and $m_j = 5$ are the initial status of λ_i and λ_j respectively on all the fibers. Each time a lightpath to be allocated a wavelength, i or j on a certain link, the value of m_i or m_j are compares and the algorithms choose the wavelength corresponding to the higher value. When used in single-fiber networks, the residual capacity is either 1 or 0; thus, the heuristic chooses the lowest-indexed wavelength with residual capacity 1. Thus, it reduces to FF.

The differences between the algorithms above is not significant, however, the FF has low complexity and small computational overhead and good blocking performance [29] and it is the algorithms used in this thesis-work.

2.2.3 PLI-RWA

In transparent networks, due to the absence of regenerators, the lightpaths QoT is degraded due to transmission impairments accumulation which should be taken into consideration while designing a network. Therefore, in addition to the availability of routes and wavelengths, an RWA technique should also consider physical layer impairments. This type of algorithms, called PLI-RWA algorithms, avoids provisioning a lightpath with an unsatisfactory QoT.

As shown in Fig. 2.1, three main approaches have been considered in [2] to handle PLI-RWA problem:

Group A

The general approach in group A is to compute the route and/or the wavelength in the traditional way and finally, verify the selected lightpath considering the physical layer impairments. The final path is chosen in a way that verifies the PLI, for instance, it should satisfy a minimum Q value or a BER threshold.

Group B

The general approach in group B considers the PLI values in the routing and/or wavelength assignment decisions. For instance, the link cost is based on the residual dispersion, the four-wave mixing, the Q-factor or the noise variance (these transmission impairments are defined in Sec. 3.2) [35]. The noise variance is the preferred one as it considers the linear and the non-linear impairments in addition to its additive nature that simplifies computation.

Group C

The general approach in group C is a combination of the two previous approaches: the PLI constraints are taken into account in the routing (case C-1), or in the wavelength assignment (case C-2) or in both (case C-3); but there is a final phase of verification of the PLI constraints that enables the re-attempt process in the lightpath selection phase.

The above verification are not only applied to the lightpath being established, however, a new lightpath with an acceptable QoT may provoke so much cross-talk impairments in the network, that QoT for another lightpath may drop below the desired threshold; thus, a good RWA algorithm should evaluate the BER of not only a candidate lightpath provided by the RWA, but also of any lightpath that the candidate lightpath might disrupt. For instance, in the MLR scenario (10 Gb/s OOK coexisting with 100 Gb/s PM-QPSK), the OOK channel can significantly degrade the performance of the already allocated PM-QPSK channel due to the XPM (detailed in Sec.3.3.1). Therefore, to avoid this problem and to have a stability, a typical approach assumes the worst-case scenario [35], which assumes that the PM-QPSK channel is in the center of the C-band

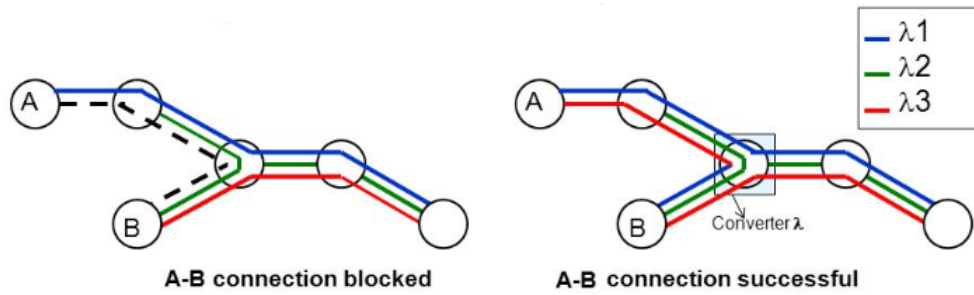


Figure 2.2: Example about fragmentation problem and the role of a wavelength converter in a network

spectrum and it is fully surrounded by OOK channels. Hence, if the lightpath's QoT is acceptable in this scenario, the actual lightpath QoT will be still acceptable even if new OOK channels are established in the network. This solution can be inefficient, since the lightpath's QoT can be estimated as unacceptable while it is not the case, however, it provides stability for the network.

2.3 Wavelength Converters in Optical Networks

After the overview above about optical network designs fundamentals, this section deals with the design of optical network including wavelength converter. Thus, it is divided in two parts: in the first part, we will define the benefits of wavelength conversion in a network, the types of wavelength converters and their required characteristics by operators and network designers are explained; in the second part, the conditions to benefit of wavelength converters in optical networks are presented.

2.3.1 Wavelength Conversion Benefits

As we mentioned in Sec. 2.1, there are two constraints to be considered when establishing a lightpath, the WCC and the clash constraints. However, these constraints results in a fragmented wavelength resource usage over the course of network operation, which leads to a low utilization network resources. The problem is illustrated by Fig. 2.2: initially, the connection from node A to node B is blocked knowing that there is a free wavelength on each of the links between the two nodes, however, they are of different indexes and consequently, the connection is blocked. In contrast, the advent of a wavelength converter in the intermediate node enabled a successful connection between the nodes A and B, by converting the wavelength of the lightpath. As a result, the wavelength converter enabled us of benefiting from the available wavelength resources. Hence, it improved the link utilization and consequently, it reduced network blocking.

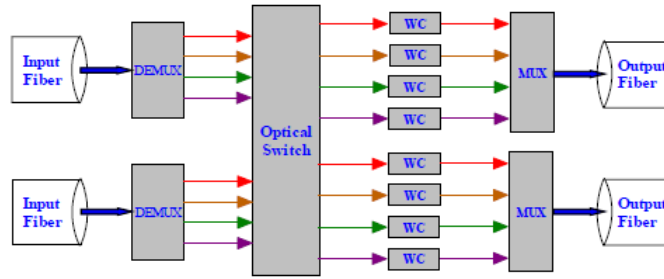


Figure 2.3: Node with complete wavelength conversion [3]

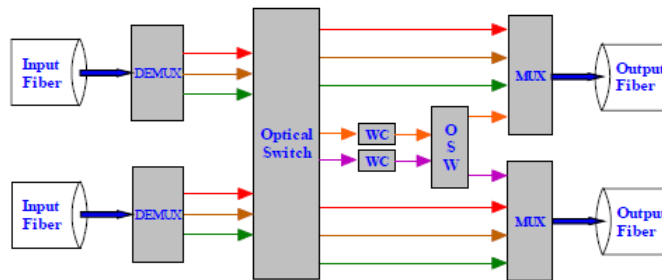


Figure 2.4: Node with partial wavelength conversion [3]

2.3.1.1 Limited and Sparse

The previous section have demonstrated the importance of wavelength converters in a network. However, they are expensive devices, thus, it is not economically possible to equip all nodes in a WDM network with these devices. If all the wavelength nodes in the network support wavelength conversion, it is called *full wavelength conversion*. However, if only a small part of the the nodes can perform wavelength conversion, the network is called with *sparse wavelength conversion* (nodes to be equipped with converters are chosen using wavelength converters placement algorithms however, this problem is not detailed in this dissertation). Moreover, the nodes supporting wavelength converters are of two types: in case each output port of the optical switch is associated with a dedicated wavelength converter, this is called *complete wavelength conversion* as shown in Fig. 2.3. Whereas, *partial wavelength conversion* is the case with limited number of converters in the node as shown in Fig. 2.4. In this work we assume full and complete wavelength conversion to simplify our work. In theses conditions, the question that may rise is : what are the requirements of theses converters to be used by networks designers and operators?

2.3.1.2 Wavelength Converters Requirements at Network Level

From a system level point of view, the features required by network operators of a practical wavelength converter in a network are [27, 28, 36]:

1. *Tuning range*: broadband tunable operation that is capable of arbitrary input and output wavelengths without any guard band.
2. *Cascadability*: high-quality operation without any degradations of the signal quality to obtain high cascadability. Wavelength converters' cascadability is the maximum number of cascaded wavelength converters that a wavelength channel can pass through without degrading its quality beyond the FEC limit.
3. *Format transparency or modulation format-agnostic*: it is the capability to convert a signal for any modulation format.
4. *Polarization independence*: since the input signal can reach the wavelength converter with any random state of polarization, the converter should not be sensitive to that.

Wavelength conversion is achieved either through the conventional opto-electronic wavelength conversion or the all-optical wavelength conversion. In the opto-electronic wavelength conversion, the optical signal is converted into the electronic domain and then reconverted to an optical signal of different wavelength [24]. The only commercially available products to do wavelength conversion are the OEO-regenerators which not only convert the signal's wavelength but also regenerate it. However, when signal regeneration is not required, these are considered expensive solution due to their high cost and energy consumption that are expected to increase as the bit-rates become higher and more advanced signal modulation technologies, with digital coherent detection such as DP-QPSK or DP-16QAM, are employed. Alternatively, authors in [37] proposed a regenerator for dual polarization QAM signals applying OEO conversion and regeneration in the digital domain without intermediate FEC. This device could be used as wavelength converter but with limited transmission reach due to the absence of FEC.

On the other hand, when using all-optical wavelength conversion, the optical signal is allowed to remain in the optical domain throughout the conversion process; there is no opto-electronic conversion. There are different approaches to perform the all-optical conversion that could be summarized as follows. The first approach is based on using wave-mixing, for example, the four-wave-mixing (FWM, defined in Sec.3.2) or difference frequency generation; the second approach is based on cross modulation, for example, the cross-gain modulation, XPM; the third approach is based on using periodically poled lithium niobate waveguide channel and cascaded second order non-linearity effect. AO-WCs based on FWM conversion schemes, which takes place in a third-order medium such

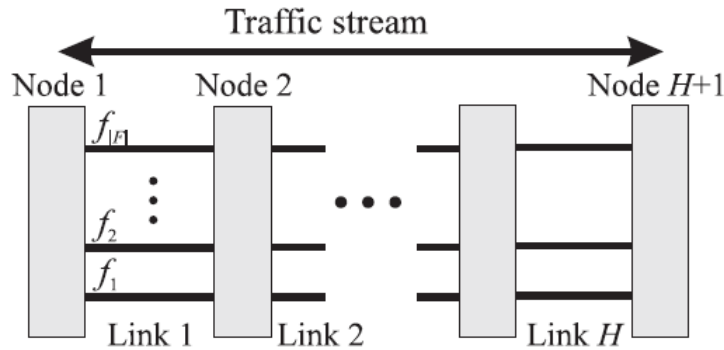


Figure 2.5: Example H-hop network with a single traffic stream using all the links [4]

as fibers, passive waveguides or active media such as semiconductor optical amplifiers, seem to be well suited for future networks as it is the only category of wavelength converters that offer a wide range of transparency to bit-rates and modulation formats [18–27] which suits the network or operators’ requirements.

2.3.2 How to Benefit From Wavelength Converters In Optical Networks

After showing the advantage of wavelength converters in terms of link utilization and how can they enhance network blocking performance, we need to understand how can we benefit from wavelength converters in optical network. Therefore, in this section, we will go through the parameters or the factors that impact the usefulness of wavelength converters in WDM optical networks:

1. Topological dependence:

In wavelength-continuous networks, the longer in hop-length H , the route between s and d , the harder to find free common wavelength to satisfy the WCC, thus, the higher the network blocking will be. That’s why the network diameter D (which is defined as the maximum over all pairs of nodes of the hop-length of their defined routes) is considered an important factor in improving network blocking performance. However, in wavelength-convertible networks, the impact of increasing D is less dramatic because a connection can access any wavelength on each link along a route. Therefore, the longer the network’s diameter, the more the divergence in performance between networks with and without wavelength conversion capability, which means an increased gain of using wavelength converters [38, 39].

However, results presented in the literature have shown that wavelength converters generally provide more significant improvements in network performance in mesh topologies than in ring topologies [38, 40], despite the fact that large ring topologies

having correspondingly large route lengths. This is because in a ring topology, a large proportion of connections which use any given link also require the use of an adjacent link, only a small proportion of connections require the use of a link without the use of the adjacent link. There are thus a large proportions of connections which use any two adjacent links in the network. Thus, it reduces the mixing of connections along routes [39], consequently reducing the need for wavelength converters. We can illustrate this effect using an extreme example of a single traffic stream offered to a multiple-hop route as depicted in Fig.2.5. If we consider an H -hop route, then each traffic stream requires the use of every link along the H -hop route. If no wavelength converters are used along the route, each lightpath is established using a common wavelength on each link. At any point in time exactly the same wavelengths are allocated to lightpaths on each link. The blocking probability experienced thus reduces to the one-hop blocking probability and wavelength converters provide no improvement in the performance.

Barry and Humblet quantified this effect using the interference length, L , which they defined as the expected number of links shared by two lightpaths which share some link [39]. In the simple example outlined here of a single traffic stream offered to an H -hop route, the interference length is $L = H$. Barry and Humblet analytically showed that for a route of fixed length, as the interference length increases, the benefit of wavelength converters decreases [16]. Moreover, they identified the *effective path length*, which is the ratio H/L , thus, as the the load mixture between links increases, L decreases. Therefore, the benefit of wavelength converters is dependent on which of the hop-length and the nodal-degree dominates in a given topology which makes it hard to predict a priori without detailed analysis [40], especially that L is dependent on the topology and the routing algorithms used [39]. Thus, in ring topology the low nodal degree dominates the high hop-length. On the other hand, for the hypercube or the fully-meshed topologies, which are highly connected, this was not valid and wavelength converters can't improve significantly the blocking performance. That's because the short hop-lengths dominates the high nodal degree [40].

Hence, using the effective path length, we can understand the previously mentioned contradiction for the ring and the hypercube or fully-meshed topologies. The former consists of large H and large L , thus, the ratio H/L is low. In the latter, the hypercube or fully-meshed topologies, have low H and low L , since it has high nodal degree that results in low-load correlation, the ratio is also low which results in a low contribution of wavelength converters. In contrast, mesh-torus topologies showed very high gain since they have relatively long routes and short L . Consequently, load-correlation is fairly low while hop-lengths are large enough so that the converters improve performance dramatically. In mesh-torus topologies, nodes are organized into two-dimensional grid where the nodes of the first and last columns are connected; it forms a torus, as shown in 25-node example in Fig. 2.6 [38]. They can be viewed as an extreme case with respect to the average number of hops required in a meshed topology, however, the benefit of wavelength

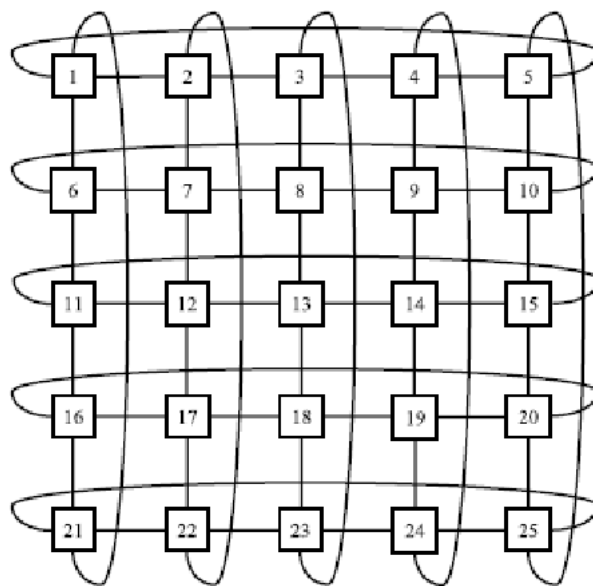


Figure 2.6: 25-node mesh torus network topology

converters may not be that huge in other meshed topologies, but as the network size increases, the blocking probability decreases very slowly in wavelength-continuous networks, whereas for wavelength-convertible network, it drops fast [38].

2. Number of wavelengths effect:

The number of wavelength is an important factor that impacts the gain of wavelength converters since the increased number of wavelengths allows increase mixing of connections [38]. Therefore, wavelength converters are more useful when the number of wavelengths per fiber is larger, especially at low load, because when the number of wavelengths is higher, the blocking is mainly due to the inability to use resources efficiently in the absence of converters and not due to the lack of resources [40].

On the other hand, as the number of wavelengths is increased, the offered load which can be supported in a network for a given blocking probability also increases. Authors in [40] estimated the benefit of wavelength converters in terms of the link utilization at a fixed blocking probability (the gain is the ratio of utilization after and before). Furthermore, they showed that the gain increases till a peak point and then starts decreasing as the number of wavelengths increases.

3. Wavelength assignment effect:

Results in [41] and [42] showed that the *most-used* algorithm performs the best among other investigated algorithms particularly in networks with high number of wavelength where increase mixing occurs, thus, a good wavelength assignment can be effective. The results were deduced in comparison to least-used, random,

and FF algorithms. The FF algorithm gives performance which is close to the performance achieved by the most-used algorithm. However, the former has an advantage over the most-used algorithm, it requires to know the state of the links on the route whereas, the most-used algorithm requires a global knowledge of the network state which makes it more computationally complex.

4. Routing algorithm effect:

It was shown that for the same network topology and traffic load, the gain in blocking or utilization (ratio of maximum offered load for wavelength-convertible and wavelength continuous networks) may be significantly different from one algorithm to another:

(a) *Alternate paths effect*

The fixed shortest-path routing algorithm minimizes the H for a given topology which reduces the effective length H/L and consequently wavelength converters gain. Therefore, using alternate-paths increases the mixing and thus, reduces L . Moreover, it increases H due to the longer paths used by demands. Furthermore, authors in [43] showed that the gain is increased as the number of the alternate paths increases. However, they showed that the benefits in blocking probability obtained by adding an alternate route (and therefore exploiting more link-disjoint paths) may be significantly more than the benefits obtained by adding (any degree of) wavelength converters in the case of fixed-alternate routing, at low loads and when the number of alternate routes between node pairs does not fully exploit the connectivity of the network topology (i.e., the number of alternate routes between node pairs is less than the edge connectivity of the network).

(b) *Dynamic routing effect*

Authors in [42] reported that dynamic routing schemes such as least-loaded routing (LLR) achieve remarkably better performance than the fixed shortest-path routing algorithm in wavelength-continuous and wavelength-convertible networks. The disadvantage of LLR algorithm is that it considers the congestion of the paths without considering hop-length and thus, it may lead to high congestion of the network at heavy load especially in wavelength-convertible networks. As a result, it will block the subsequent demands requiring short paths. Therefore, to handle this trade-off, Li et. al. [44–46], proposed an algorithm called weighted-least-congested-route (WLCR) which considers the distribution of free wavelengths and the hop length of each route jointly thus, the path weight is proportional to the number of free wavelengths in the route and inversely proportional to its length. Consequently, among set of routes between s and d , WLCR chooses the route with the highest weight. WLCR outperformed LLR, fixed-alternate routing and fixed shortest-path routing algorithms due to the balance it provides between the length of the path and its congestion while making the routing decision.

5. Network conversion density:

In the previous sections, the main assumption was full wavelength conversion, however, this is not a realistic assumption since wavelength converters are expensive devices and they are usually only put on few nodes. Therefore, authors in [40] modeled a network with sparse wavelength conversion assuming that a node is capable of wavelength conversion with probability q , the conversion density of the network, to study the effect of q on the performance enhancement using 11×11 and 101×101 node bidirectional mesh-torus network. The conclusions show that the blocking probability drops more steeply with the conversion density as the number of wavelengths increases. The advantage of wavelength conversion are much higher in a larger network and as network size increases, performance increases dramatically initially with conversion density. For example, in the 101×101 node topology case, having number of wavelengths to be 5, a decrease in blocking probability of two orders of magnitude occurs as the conversion density increases from 0 to 0.2. In contrast, as the number of wavelength increases up to 8, a decrease in blocking probability of two orders of magnitude occurs as the conversion density increases from 0 to 0.1. This not only suggests that having a converter at every node of the network may be unnecessary to achieve a given performance, but also the proportion of converter nodes required is a function of the size of the network and the number of wavelengths per fiber. Finally, in this thesis-work, we will consider that each node is equipped with unlimited number of AO-WCs to simplify the assumption. In other words, to avoid solving the wavelength converter placement problem, we assume complete and full wavelength conversion scenarios.

6. AO-WCs' limitations:

AO-WCs are limited in terms of tuning range and cascadability which degrade optical networks' performance enhancement. Therefore, these limitations should be considered while solving the RWA in order to decrease their impact on the gain wavelength converters can contribute. Up to our knowledge, there is no study that considers the effect of AO-WCs' conversion range and cascadability except in [23, 24]. Their study aimed to take advantage of an AO-WC's unique multi-wavelength conversion (can convert multiple channels simultaneously) capability to maximize converter sharing. The results showed that, to have the same network blocking performance as in the case of OEO-WC, the maximum number of cascaded converters needed is four for the CORONET topology while it is only two for the Japan topology. The input bandwidth is 1000 GHz and the maximum amount to shift equals 1400 GHz. Moreover, the study shows that using multi-wavelength conversion AO-WCs resulted in a 60% reduction of the total number of converters needed and doubled the resource utilization at 5% of network blocking.

2.4 Conclusion

In this chapter, we have introduced the fundamentals of optical networks design which aims to find routes and allocating resources (RWA) for traffic demands that are either known beforehand (static traffic assumption) or arrives sequentially and occupy resources for a deterministic period (dynamic traffic assumption). RWA is considered NP-complete problem and thus, the time required to find an optimal solution for such problems increases exponentially as the size of the problem increases. Therefore, heuristic algorithms that find sub-optimal solutions are preferred due to their simplicity. Moreover, RWA is decoupled in two sub-problems, the routing sub-problem and the wavelength allocation sub-problem where we have shown different approaches and heuristics used to solve each of them. Additionally, since we are assuming transparent optical network, the QoT of the lightpath should be considered before establishing the lightpath and this recalls for what's called physical layer impairment aware RWA (PLi-RWA) where we have shown different approaches to handle this problem.

In the second section, we have presented wavelength convertible networks design. It started by the required characteristics of AO-WCs in order to be accepted by network designers and operators and the different approaches to design AO-WCs. Afterwards, we have presented an overview about the conditions of benefiting from wavelength converters in optical networks which are as follows: the network topology, the number of wavelengths per fiber, the number of alternative paths between source and destination of traffic demands, wavelength assignment algorithms and routing algorithms. Therefore, the target of this thesis is to investigate which of these factors enables AO-WCs to result in a network performance enhancement as OEO-WCs especially that AO-WCs add constraints regarding their limitations (tuning range and cascability) that should be taken into consideration while designing the network.

Chapter 3

Transmission Layer Model

3.1 Introduction

In transparent optical networks, the optical signal is not regenerated at the intermediate nodes over the route and hence, PLIs accumulation may result in an unacceptable QoT of the lightpath at the receiver. Therefore, a performance prediction tool is used to estimate the lightpath performance and confirm its QoT before establishing it. In this thesis-work, we have used two different transmission layer models based on two different categories of modulation formats and bit-rates and thus, dominating PLIs correspond to two stages. In the first stage of this thesis, during building our first network model, based on offline traffic assumption, upgrading network to increase its capacity by including the 100 Gb/s PM-QPSK to their infrastructure without losing the legacy 10 Gb/s OOK. This is known as MLR network [5, 35, 47–51] where the 10 Gb/s OOK is based on direct detection and hence, unlike the 100 Gb/s PM-QPSK where fibers chromatic dispersion (CD) compensation is done electronically, dispersion compensating fibers (DCFs) are used for this goal and hence, we call it *the compensated transmission model*. On the other hand, due to the exponential increase of network traffic, operators are moving towards 400 Gb/s links [1], thus, when we have started the second stage of this work, which is the operational phase based on the online simulation, we found the need to move towards using higher-order modulation formats based on elastic transponder [16]. Therefore, in this latter scenario, all the formats are based on coherent detection and electronics CD compensation which makes no need for DCFs. This is known as *uncompensated-transmission* [52, 53].

This chapter is organized as follows: Sec. 3.2 includes a brief overview and definitions of the transmission layer impairments. Afterwards, Sec. 3.3.1 and Sec.3.4 describe the models of the compensated and uncompensated transmissions.

3.2 Transmission Impairments

Physical layer impairments can be classified into linear and nonlinear effects. Linear impairments are independent of the signal power and affect each of the wavelengths (optical channels) individually, whereas nonlinear impairments affect not only each optical channel individually but they also cause disturbance and interference between them [2, 54].

3.2.1 Linear impairments

The important linear impairments are:

Fiber attenuation, amplifier spontaneous emission (ASE) noise, chromatic dispersion (CD) or group velocity dispersion, GVD and polarization mode dispersion (PMD). They are defined as follows:

Fiber attenuation:

The signal power traveling along the fiber decreases exponentially with increasing distance. The attenuation coefficient α is expressed in dB per unit length. For typical fiber optic communication systems working at 1530 to 1570 nm (191-196 THz), the attenuation coefficient of single-mode fiber (SMF), the most widespread optical fiber in the world, is 0.2 dB/km. Fiber attenuation losses are compensated by using EDFA optical amplifiers.

ASE:

EDFAs are used in fiber optic communication systems to compensate for attenuation and components' insertion losses. However, they result in ASE noise which is generated by spontaneous decay of electrons in the upper energy levels to lower energy levels in the atoms of Erbium doped material [54]. This results in the emission of photons in a wide frequency range. The amplifier noise is quantified by noise figure value, which is the ratio of the OSNR before the amplification to the same ratio after the amplification and is expressed in dB.

Single-span optically amplified systems are characterized by an optical amplifier at the receiver input, called pre-amplifier which has a high gain in order to obtain a high power at the photodiode input. Therefore, the performance depends exclusively on the optical pre-amplifier ASE noise, that turns out to be: Gaussian, white (over the well-known C-band that ranges between 1530 and 1570 nm or 191-196 THz) and additive on the input optical field. When using only one amplifier at the end of the link, the Rx received power decreases exponentially as a function of fiber length. As a result, the maximum reach cannot be very long (a few hundreds of km at best). Therefore, if we want to go further, we need to use in-line amplifiers which is also known as multi-span system. The ASE noise at the end of the system

is the accumulation of all the generated ASE noises at each span. Therefore, the maximum number of spans is defined by the required OSNR at the receiver.

CD:

CD causes pulse broadening in the time domain, thus, it results in interference among consecutive pulses and it is called the inter-symbol-interference which affects the receiver performance by spreading the pulse energy beyond the allocated bit slot. The time delay accumulated over a certain distance, by two spectral components, is described by the GVD parameter β_2 (the second order derivation of the propagation constant β), however, in fiber optic communication, dispersion parameter D is a more commonly used parameter for expressing the propagation delay among two pulses. D is related to β_2 as follows:

$$D = -\frac{2\pi c}{\lambda^2}\beta_2 \quad (3.1)$$

where λ is wavelength of the carrier signal and c is the speed of light in vacuum. D and β_2 have units of ps/(nm-km) and $s^2 m^{-1}$ respectively, the typical value of D is 17 dB/km ps/(nm-km) when SMF is used. A countermeasure to the dispersion is to compensate dispersion, using negative-dispersion fibers. Therefore, when the accumulated dispersion is zero, there is no distortion, the signal is fully recovered.

PMD

Optical fibers have irregular core radius or shape along the fiber length and thus, it results in randomly varying difference among the refractive indices of two principle states of polarization of the fiber. Therefore, the light propagates with different velocities in the two axes and the signal broadens along the propagation [54]. This is called the PMD.

The effect of PMD is accounted for with an OSNR penalty [35]. However, due to the stochastic nature of PMD, the penalty related to a given value of mean DGD which is defined:

$$\Delta\tau_{RMS} = D_p\sqrt{L} \quad (3.2)$$

where $\Delta\tau_{RMS}$ is the mean DGD and D_p is the PMD parameter expressed in picoseconds per square root of kilometers of fiber length L . D_p has typical values of 0.01-1 ps/ \sqrt{km} .

3.2.2 Non-linear Impairments

Nonlinear effects in optical fibers occur due to (1) change in the refractive index of the medium with optical intensity and, (2) inelastic scattering phenomena. These nonlinearities are defined as follows [55, 56]:

3.2.2.1 Inelastic Scattering

At high power level (beyond few tenths of mwatts), the inelastic scattering phenomenon can induce stimulated effects such as Stimulated Brillouin Scattering (SBS) and Stimulated Raman Scattering (SRS). The intensity of scattered light grows with the incident power. The difference between Brillouin and Raman scattering is that the Brillouin generated photons (acoustic) are coherent and give rise to a macroscopic acoustic wave in the fiber, while in Raman scattering the phonons (optical) are incoherent and no macroscopic wave is generated. These impairments set an upper limit on the amount of optical power that can be emitted into an optical link [55, 56].

3.2.2.2 Nonlinear Refractive Index Effects

The power dependence of the refractive index is responsible for the Kerr-effect which leads to nonlinear phase shift. Depending upon the type of input signal, the Kerr-nonlinearity manifests itself in three different effects such as:

Self-Phase Modulation (SPM):

In a medium that has an intensity-dependent refractive index, the higher intensity portions of an optical pulse encounter a higher refractive index of the fiber compared with the lower intensity portions while it travels through the fiber. This refractive index change results in a phase change and since this nonlinear phase modulation is self-induced, the nonlinear phenomenon resulted is called SPM.

For phase modulated optical communication systems, SPM manifests itself as the rotation of constellation from its original position. At the receiver the rotated constellation points are erroneously decoded and become source of penalty [54]. Moreover, phase modulation of signals due to SPM converted to intensity modulation through dispersion and thus results in waveform distortions.

Cross-Phase Modulation (XPM):

The refractive index not only varies with the power of the central channel but also with the power in the neighboring channels in a nonlinear fashion, thus, XPM is the modulation of the signal phase that is proportional to the power of the signal in the neighboring channels in a WDM systems [54].

The main limitation of quadrature phase shift keying (QPSK) operated in a hybrid scenario, i.e., with two or more different formats mixed on the WDM comb, lies in its limited tolerance to XPM caused by neighboring intensity-modulated OOK channels. The impact XPM is usually decreased by increasing the channel spacing, introducing guard-band between QPSK and OOK channels or decreasing the power of the OOK channel [35, 57].

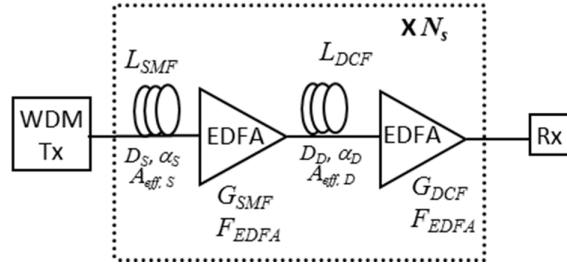


Figure 3.1: Point-to-point link schematic

Four-Wave Mixing (FWM):

The FWM process originates as follows, if three optical fields with carrier frequencies ω_1 , ω_2 and ω_3 , copropagate inside the fiber simultaneously, they generate a fourth field with frequency ω_4 , which is related to other frequencies by a relation, $\omega_1 + \omega_2 = \omega_3 + \omega_4$.

SPM and XPM are significant mainly for high bit rate systems, but the FWM effect is independent of the bit rate and is critically dependent on the channel spacing and fiber dispersion. Since the dispersion varies with wavelength, the signal waves and the generated waves have different group velocities. This destroys the phase matching of interacting waves and lowers the efficiency of power transfer to newly generated frequencies. The higher the group velocity mismatch and wider the channel spacing, the lower the four wave mixing [55, 56].

Performance estimation models should take into account these impairments as will be shown in the next sections.

3.3 Compensated Transmission

To meet the explosive transmission requirements in the backbone network based on WDM, the channel's rate is increased from 10 Gb/s using OOK to higher bit-rates by introducing different modulation formats such as: 40 Gb/s differential quadrature phase-shift keying (DQPSK) and 100 Gb/s PM-QPSK [35, 58] using the conventional channel bandwidth and spacing [59]. However, due to different traffic demands, some lightpaths may not require the 100 Gb/s rate hence, MLR networks should be supported for cost-efficient networks to provision various demand flexibly [60]. The disadvantage of the MLR scenario is that the OOK and xQPSK channels coexist on the same physical fiber which will result in XPM that will mainly degrade the xQPSK performance and thus, it should be well studied while designing the links. Therefore, in this section, we will show the MLR model used to estimate the performance of each modulation modulation taking into account all the PLIs.

Table 3.1: The characteristics of fiber used [5]

Fiber type	α (dB/km)	D (ps/nm.km)	A_{eff} (μm^2)	L_s (km)
SMF	0.23	17.1	80	80
DCF	0.5	-92	20	15

3.3.1 MLR Model

The lightpath QoT is measured using the bit-error-rate (BER) which is computed using the Gaussian approximation as defined follows [35]:

$$BER = \frac{1}{2} \operatorname{erfc} \left(\frac{Q}{\sqrt{2}} \right) \quad (3.3)$$

where Q is the Q-factor that depends on the modulation format used by the lightpath and is calculated in the following sections. However, before we go in details about how to calculate Q-factor, we need to show how the OSNR is calculated in this model since it will be needed afterwards.

3.3.1.1 OSNR Calculation

In compensated transmission links, every span includes a SMF and DCF to compensate for the fiber CD characterized as shown in Tab. 3.1, where L , α , D and A_{eff} are fiber length, fiber attenuation, fiber CD and fiber effective area. Moreover, to compensate fiber attenuation losses, each fiber is followed by an EDFA amplifier as shown in Fig. 3.1. However, EDFA contributes by the ASE noise and thus, the OSNR at the receiver nodes becomes as follows:

$$OSNR = \frac{P_{ch}}{N_s \cdot P_{ASE}} \quad (3.4)$$

where P_{ch} is the channel's average optical power, N_s is the number of spans between two nodes and P_{ASE} is the ASE noise contributed by a single span is calculated as follows:

$$P_{ASE} = h \cdot f_0 \cdot F \cdot B_{ref} \cdot ((G_{SMF} - 1) + (G_{DCF} - 1)) \quad (3.5)$$

where F is the noise figure, h is Planck's constant, f_0 is the C-band center frequency, G_{SMF} and G_{DCF} are the amplifiers gain, which compensate exactly for the fiber losses, and $B_{ref} = 12.5$ GHz is the reference bandwidth (equivalent to 0.1 nm) at which the OSNR is measured at the receiver. Now, using this OSNR, we will show how is the lightpath Q-factor is calculated for different modulation formats.

3.3.1.2 OOK BER Estimation

In the case of OOK, the most relevant impairments are ASE, CD, GVD, SPM and XPM [35]. SPM and XPM interplay with chromatic dispersion cannot be avoided in practice through engineering rules. Hence, cumulative criteria have to be found to assess the amount of SPM and XPM. For this purpose, authors in [61] have chosen to use the NL phase ϕ_{NL} , which is the average phase variation due to Kerr effect. Therefore, criteria chosen are OSNR, the PMD coefficient, the residual dispersion d_{res} and ϕ_{NL} . Uncompensated PMD is not an issue for most type of fibers at 10 Gb/s, however it becomes an issue at 40 Gb/s or higher bit-rates [2, 35]. BER is linked to the remaining parameters using the Q-factor that is calculated as follow [61]:

$$Q = Q' \cdot \sqrt{OSNR} \cdot \sqrt{\frac{B_{ref}}{B_e}} \quad (3.6)$$

where B_e is the electrical bandwidth of the receiver, around 7.5 GHz for 10 Gb/s with FEC. Q' ranges from 0% to 75%, it's depending on the residual dispersion d_{res} and the average phase variation due to Kerr effect ϕ_{NL} and it was obtained as an average of 60,000 simulations.

3.3.1.3 xQPSK BER Estimation

The evaluation of BER for PM-QPSK and DQPSK signals, affected by Additive White Gaussian Noise (AWGN) and phase noise, involves the evaluation of an infinite series of Bessel function which require high computational operations. On the other hand, a very accurate but much simpler approximation can also be obtained by observing that, in QPSK systems, errors occur when the received phase, affected by nonlinear phase noise and AWGN, differs from the transmitted one by more than $\pi/4$. Since the nonlinear phase noise due to SPM and XPM is modeled as a Gaussian phase noise with variance σ_{NL}^2 , thus, the Q-factor due to ASE and phase noise is defined as [35]:

$$Q = \frac{\pi/4}{\sqrt{\frac{k}{2\rho} \left(\frac{\theta}{\sin(\theta)}\right)^2 + \sigma_{NL}^2}} \quad (3.7)$$

where $k=1, 2$ for PM-QPSK and DQPSK respectively, ρ is the signal to noise ratio (SNR) per symbol related to OSNR by:

$$\rho = n \cdot B_{ref} \cdot T \cdot OSNR \quad (3.8)$$

where $n=1, 2$ is the ratio between the number of noise and signal polarization for PM-QPSK and DQPSK respectively, $T=40, 50$ ps is the symbol time for PM-QPSK and

DQPSK respectively. θ is the angle for which the contribution of AWGN to the distribution of the total phase around $\pi/4$ is maximum, is defined as follows:

$$\theta = \frac{\pi/4}{k + 2\rho\sigma_{NL}^2} \quad (3.9)$$

where the Gaussian phase noise variance σ_{NL}^2 constitutes of the noise variances due to SPM and XPM as follows:

$$\sigma_{NL}^2 = \sigma_{SPM}^2 + \sigma_{XPM}^2 \quad (3.10)$$

where σ_{SPM}^2 is defined as [62, 63]:

$$\sigma_{SPM}^2 \simeq \frac{a \cdot \langle \phi_{SPM,SMF}^2 \rangle}{(3\rho)} + \frac{a \cdot \langle \phi_{SPM,DCF}^2 \rangle}{(3\rho)} \quad (3.11)$$

where $\langle \phi_{SPM}^2 \rangle$ is the average nonlinear phase shift is defined as:

$$\langle \phi_{SPM}^2 \rangle = N_s \cdot \gamma \cdot L_{eff} \cdot P_{ch} \quad (3.12)$$

where, $a = 4, 2$ for DQPSK and PM-QPSK respectively and L_{eff} is the effective length. Hence, using eq. 3.11 we calculate the variance of the nonlinear phase shift due to SPM [35]. On the other hand, σ_{XPM}^2 (the second part of eq. 3.10) is the variance of the nonlinear phase shift due to XPM at the destination node and therefore, it is the accumulation of XPM along the spans which is either a coherent or incoherent accumulation [35]. When an independent interfering OOK channel j contributes to XPM at different spans due to add/drop of channels, in this case, XPM accumulates incoherently (randomly). On the other hand, when an interfering channel j is present along the whole path, i.e. no add/drop is performed at the wavelength, XPM accumulates coherently. The latter case is the most pessimistic since the variance grows quadratically with the number of spans and make it unfeasible the coexistence of xQPSK channels and OOK channels, whereas, in the incoherent accumulation, which is the most realistic scenario, XPM grows linearly and thus, it is the assumption we will use in this thesis-work. Accordingly, XPM at the receiver becomes:

$$\sigma_{XPM}^2 = \sum_j \cdot \sigma_j^2 \quad (3.13)$$

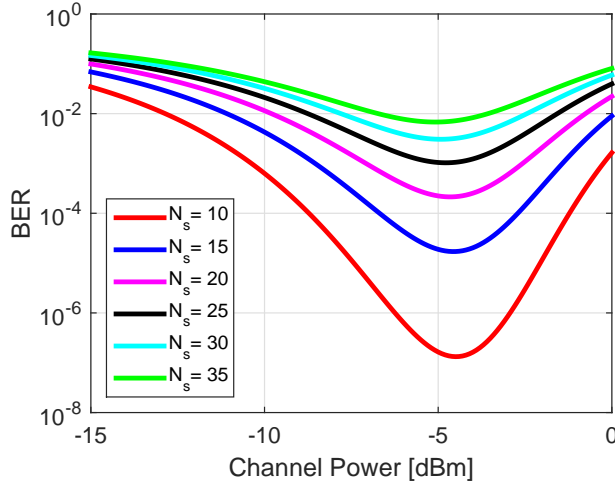
where σ_j^2 is defined as follows:

$$\sigma_j^2 = \sum_i \sigma_{i-span,j}^2 \quad (3.14)$$

where $\sigma_{i-span,j}^2$ is the XPM contribution of interfering OOK channel j , in span i , which consists of SMF and DCF fibers, thus, it is defined as:

$$\sigma_{i-span,j}^2 = \sigma_{i-SMF,j}^2 + \sigma_{i-DCF,j}^2 \quad (3.15)$$

where $\sigma_{i-SMF,j}^2$ and $\sigma_{i-DCF,j}^2$ are the XPM contributions in the SMF and DCF fibers respectively. Finally, $\sigma_{i-span,j}^2$ is calculated as per equation (9) of [35].

Figure 3.2: BER vs P_{ch} for different number of spans

3.3.2 System Performance

The performance of xQPSK channels mainly depend on σ_{NL} which is dependent on: N_{ch} , the number of OOK channels surrounding PM-QPSK or DQPSK, the channel spacing Δf , the fiber and DCF characteristics, the number of spans in the point-to-point link N_s and finally the channels average optical power. However, the fiber types used are SMF and DCF characterized as shown in Tab. 3.1 and $\Delta f = 50$ GHz [59], hence, the optimum channel power, $P_{ch,opt}$, is dependent on N_{ch} and N_s .

To find the $P_{ch,opt}$, we plot the BER, calculated using the Gaussian approximation, of a lighthpath, assuming it's using PM-QPSK, versus the P_{ch} for multiple values N_s and fixed $N_{ch} = 80$ as shown in Fig. 3.2 which is analyzed as follows. The plots show that BER decreases as the power of the channel is increased until a minimum point and then, it starts increasing again; this performance is due to non-linearity. The $P_{ch,opt}$ is almost the same for any N_s . Therefore, we are left with the number of channels to decide the $P_{ch,opt}$.

For that purpose, we plot BER of a light path using PM-QPSK versus P_{ch} for multiple values of N_{ch} and fixed value of $N_s = 25$ as shown in Fig. 3.3. Conclusions could be driven are as follows: increasing the number of channels leads to significant degradation in BER and variation in the $P_{ch,opt}$ as well. Thus, for a stable design, we will use the worst-case assumption where we assume that the link is fully loaded of OOK channels with a central PM-QPSK channel (or DQPSK). It is true that this is a pessimistic assumption, however, any change in the number of OOK channels is already considered and will not affect the performance of already established lighthpaths using xQPSK. Finally, having the number of channels fixed, we need to find the $P_{ch,opt}$. For that purpose, we plot in

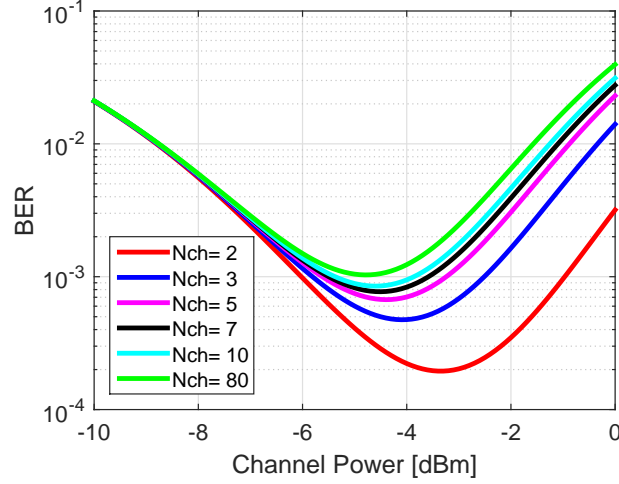


Figure 3.3: BER vs P_{ch} for different number of channels

Fig. 3.4 the maximum possible N_s that a lightpath can reach satisfying the FEC limit versus P_{ch} using different modulation formats. The result shows that $P_{ch,opt} = -4\text{dBm}$ is the required operational power that we will use.

3.4 Uncompensated Transmission Model

Uncompensated transmission are less impacted by non-linearity than dispersion-managed links and thus, made it possible to use multi-level modulation formats with polarization multiplexing which increased system spectral efficiency [52, 53]. To understand the behavior of uncompensated transmission, certain perturbative models of fiber non-linear propagation can provide accurate system performance prediction. In this thesis-work we will be using the Gaussian-noise (GN) model which had proved itself a relatively simple and sufficiently reliable at the same time for performance prediction over wide range of system scenarios, effective for both system analysis and design [52, 53, 64]. Therefore, in this section, we introduce the GN-model, its assumptions, validations and limitations and define the formulas and equations that will benefit our work to estimate the point-to-point link performance.

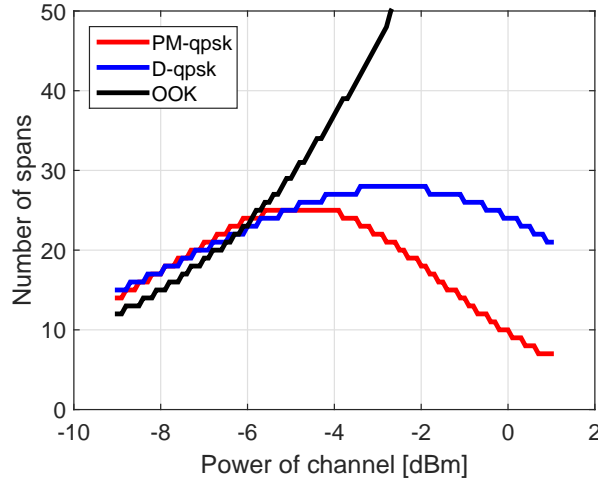


Figure 3.4: Maximum number of spans reached by each modulation format versus P_{ch} at BER= 10^{-3}

3.4.1 GN-model

3.4.1.1 Validation and Limitations

The GN-model is based on certain assumptions and have some limitations as shown below, otherwise it need to be confirmed. One of the most pillars is assuming that non-linear-interference (NLI) noise is approximately Gaussian and additive [52,65]. Moreover, an important limitation is that signal is assumed to be Gaussian itself, which requires accumulated dispersion and symbol rate to be large enough. This makes the prediction in single span inaccurate. Therefore, in order to have reliable predictions, the following limitations need to be considered:

1. Symbol Rate $R_s \geq 28$ GBaud.
2. Channel spacing ≤ 100 GHz.
3. $N_{ch} \geq 3$ channels.
4. Dispersion (D) ≥ 2 ps/(nm.km).
5. $N_{spans} > 1$ span.

3.4.1.2 GN-model Reference Formula

The GN-model reference formula provides $G_{NLI}(f)$, that is the NLI noise power-spectral-density (PSD) at the end of the link. The following version was derived based on three main assumptions: 1)the transmitted signals are dual-polarization; 2)a span consists of a single fiber type; 3)the links are homogeneous (made up of identical spans) and transparent (the loss of each span is totally compensated by the the optical amplifier). As a result, the NLI's PSD generated at frequency f :

$$G_{NLI}(f) = \frac{16}{27}\gamma^2 L_{eff}^2 \cdot \int_{-\infty}^{\infty} \int_{-\infty}^{\infty} G_{WDM}(f_1)G_{WDM}(f_2)G_{WDM}(f_1 + f_2 - f) \cdot \rho(f_1, f_2, f) \cdot \chi(f_1, f_2, f)df_2df_1 \quad (3.16)$$

It can be physically interpreted as describing the beating of each thin spectral slice of the WDM signal with all other FWM processes, where $\rho(f_1, f_2, f)$ is the FWM efficiency of the beating of the 3 pump frequencies f_1, f_2 and $f_3 = f_1 + f_2 - f$ creating an interfering frequency at f for the lumped amplification case and thus, it is defined as:

$$\rho(f_1, f_2, f) = \left| \frac{1 - e^{-2\alpha L_s} e^{j4\pi^2\beta_2 L_s (f_1 - f)(f_2 - f)}}{\alpha - j4\pi^2\beta_2 (f_1 - f)(f_2 - f)} \right|^2 \cdot L_{eff}^2 \quad (3.17)$$

$\chi(f_1, f_2, f)$ takes into account coherent interference at the receiver location on NLI produced in each span defined as:

$$\chi(f_1, f_2, f) = \frac{\sin^2(2N_s\pi^2(f_1 - f)(f_2 - f)\beta_2 L_s)}{\sin^2(2\pi^2(f_1 - f)(f_2 - f)\beta_2 L_s)} \quad (3.18)$$

where $G_{WDM}(f_1) \cdot G_{WDM}(f_2) \cdot G_{WDM}(f_1 + f_2 - f)$ represents the PSD i.e., the strength that each of three pumps carries; α is fiber attenuation coefficient [km^{-1}] such that the signal power is attenuated as $\exp(-2\alpha L_s)$; β_2 is the absolute value (always positive) of dispersion in [$\text{ps}^2 \text{km}^{-1}$]; γ is fiber non-linearity coefficient [$\text{W}^{-1} \text{km}^{-1}$]; L_s is the span length [km]; L_{eff} is the effective length [km], defined as $[1 - \exp(-2\alpha L_s)]/\alpha$; N_s : is the link total number of spans.

3.4.1.3 Analytical Closed-Form Formula

In the general case, the reference formula can not be solved analytically, thus, closed-form approximate formulas, that help in carrying out performance assessment in wavelength-routed network, were derived in [52] based on different assumptions:

I Ideal Nyquist-WDM over single span

The term 'ideal Nyquist-WDM' means a system whereby each channel has a perfectly rectangular spectrum of width equal to R_s and the channel spacing also

coincides with R_s . Additionally, the amplification should be lumped, which means an optical amplifier that compensate for the fiber losses is placed at the end of the span.

II Non-Nyquist-WDM over single span

The assumptions in this approximation are as follows. Lumped amplification at the end of the span and transparency. An equal number of channels to the left and right of the center channel where all channels are identical. It starts causing non-negligible error if the spans <10 dB. The derivation assumes rectangular spectra, otherwise, going from spectra to raised-cosine with roll-off 0.3, causes an error up to 0.3 dB. Finally, the the error is decreased more as the symbol rate goes higher than 25 GBaud. Then, the NLI PSD at the center of the center channel is approximately:

$$G_{NLI}(0) \approx \frac{8}{27} \gamma^2 G_{WDM}^3 L_{eff}^2 \frac{\operatorname{asinh} \left(\frac{\pi^2}{2} \beta_2 L_{eff,a}^2 B_{ch}^2 N_{ch}^2 \frac{B_{ch}}{\Delta f} \right)}{\pi \beta_2 L_{eff,a}^2} \quad (3.19)$$

where B_{ch} is the -3 dB bandwidth of each channel and Δf is the channel spacing. This approximation fits with this thesis-work and it will be the assumption we use in estimating the link performance.

III Whole system solver

In reality, it is hard to fulfill the homogeneous and transparency assumptions. Moreover, channels may have different launch power, symbol rates and uneven spacing. Thus, the 'whole system solver' approximation can accommodate the all these diversities provided that the incoherent GN-model or IGN-model (will be detailed in the next section) of incoherent accumulation is accepted. This formula still provides reasonably reliable results, typically to within 1.5 dB of accuracy versus the GN-model reference formula [52].

3.4.2 IGN-model

The GN-model reference formula accounts for the coherent interference that occurs at the Rx among the NLI generated in each single span. On the other hand, an alternative model which coincides with the GN-model over each single span but makes the further approximation of completely neglecting coherent interference among NLI generated in different spans is called the incoherent GN-model, or IGN-model. According to it, the total NLI PSD at the end of the link is simply:

$$G_{NLI}^{inc}(f) = \sum_{n=1}^{N_s} G_{NLI}^n(f) \quad (3.20)$$

where $G_{NLI}^n(f)$ is the NLI PSD generated in the n^{th} span alone, then propagated through the link all the way to the Rx. In case the links are transparent and homogeneous, thus

the NLI PSD becomes:

$$G_{NLI}^{inc}(f) = G_{NLI}(f) \cdot N_s \quad (3.21)$$

3.4.3 System Performance

The performance of optical coherent systems or the QoT is decided b means of BER which is linked to the OSNR. The later is calculated using the previous approximations of the GN-model reference formula. Moreover, in the GN-model, NLI noise is assumed to be Gaussian and additive [52, 65], similar to ASE. additionally, ASE and NLI are assumed to be uncorrelated, therefore, their power could be added at the denominator of the OSNR, which becomes:

$$OSNR = \frac{Pch}{P_{ASE} + P_{NLI}} \quad (3.22)$$

where P_{ASE} is the total ASE noise power at the end of the link calculated using eq. 3.5 but considering only the ASE noise generated from one amplifier that compensates for dber losses since DCFs are not used in the uncompensated transmission and thus, their corresponding amplifier are not needed, hence, P_{ASE} becomes:

$$P_{ASE} = N_s \cdot P_{ASE}^{(1)} = N_s \cdot h \cdot f_0 \cdot F \cdot B_{ref} \cdot (G - 1) \quad (3.23)$$

where $P_{ASE}^{(1)}$ is the ASE power generated for a single span. P_{NLI} is the NLI power which could approximated, if the $G_{NLI}(f)$ is assumed locally white across the bandwidth, similar to ASE noise. This approximation has an almost negligible impact on the main system performance as shown in [52], it simplifies the performance estimation since it would require estimating $G_{NLI}(f)$ at only one frequency:

$$P_{NLI} = G_{NLI}(f) \cdot R_s = N_s \cdot \eta^1 \cdot P_{ch}^3 \quad (3.24)$$

where $\eta^{(1)}$ is the non-linearity PSD for a single span, it is a power-independent coefficient. The form on the right is used for link optimization and finding the channel's optimal power; thus, assuming the IGN approximation, $\eta^{(1)}$ is calculated as follows:

$$\eta^{(1)} = \frac{P_{NLI}^{(1)}}{P_{ch}^3} = \frac{8}{27} \gamma^2 L_{eff}^2 \frac{\operatorname{asinh} \left(\frac{\pi^2}{2} \beta_2 L_{eff,a}^2 B_{ch}^2 N_{ch}^2 \frac{B_{ch}}{\Delta f} \right)}{\pi \beta_2 B_{ch}^2 L_{eff,a}^2} \quad (3.25)$$

$P_{NLI}^{(1)}$ and $\eta^{(1)}$ are the NLI power and coefficient at the end of a single span. Therefore, using all the above derivations, the final form of the OSNR, assuming the 'Non-Nyquist-WDM over single span' approximation, is as follows:

$$OSNR = \frac{Pch}{N_s \cdot P_{ASE}^{(1)} + N_s \cdot \eta^{(1)} P_{ch}^3} \quad (3.26)$$

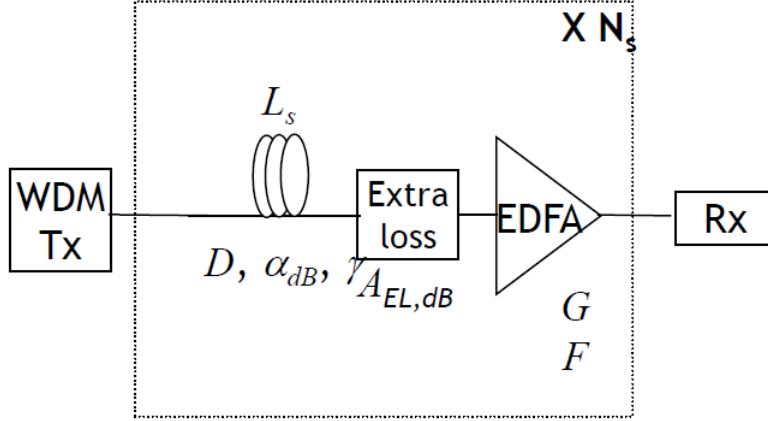


Figure 3.5: Point-to-point link schematic

Using OSNR calculated in Eq. 3.26, the expected BER at the receiver is calculated as follows:

$$BER_{PM-BPSK} = \frac{1}{2} \operatorname{erfc} \left(\sqrt{OSNR} \right) \quad (3.27)$$

$$BER_{PM-QPSK} = \frac{1}{2} \operatorname{erfc} \left(\sqrt{\frac{OSNR}{2}} \right) \quad (3.28)$$

$$BER_{PM-16QAM} = \frac{3}{8} \operatorname{erfc} \left(\sqrt{\frac{OSNR}{10}} \right) - \frac{9}{64} \operatorname{erfc}^2 \left(\sqrt{\frac{OSNR}{10}} \right) \quad (3.29)$$

$$BER_{PM-64QAM} = \frac{7}{24} \operatorname{erfc} \left(\sqrt{\frac{OSNR}{42}} \right) - \frac{49}{384} \operatorname{erfc}^2 \left(\sqrt{\frac{OSNR}{42}} \right) \quad (3.30)$$

where $BER_{PM-BPSK}$, $BER_{PM-QPSK}$, $BER_{PM-16QAM}$ and $BER_{PM-64QAM}$ corresponds to the BER of the lightpaths using PM-BPSK, PM-QPSK, PM-16QAM or PM-64QAM respectively. The higher the modulation format to be used, the higher the required OSNR. The latter is affected by the fiber's non-linearity, P_{ASE} and P_{ch} , however, in this work the fiber used is SMF (characterized as written in Tab. 3.1), the span length is 100 km preceded by an EDFA optical amplifier that compensates for fiber losses as shown in Fig. 3.5, the channel spacing is $\Delta=50$ GHz as per the ITU standards [59], the symbol rate is $R_s=32$ GBaud and consequently the channel's bandwidth is:

$$B_{ch} = (1 + m) \cdot R_s \quad (3.31)$$

where m is the roll-off assuming raised cosine signal spectrum. Therefore, to find the channel's optimum power, $P_{ch,opt}$, we are left with the number of spans N_s and number of channels in the fiber N_{ch} .

First of all, we assume that all the channels have the same power in order to use the Non-Nyquist-WDM over single span approximation. The number of channels is fixed to

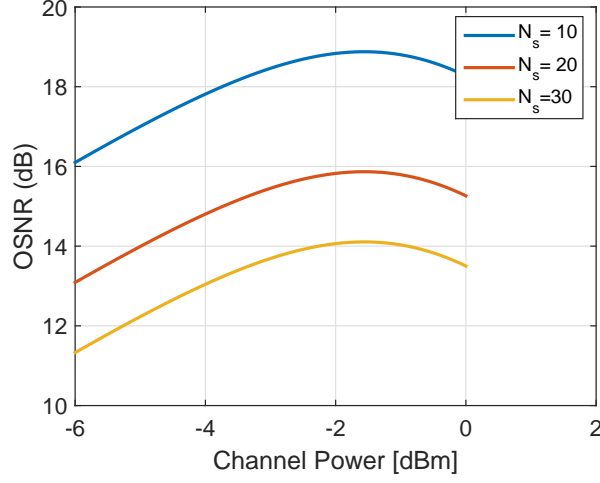


Figure 3.6: OSNR vs P_{ch} for different N_s

$N_{ch}=80$, then, in Fig. 3.6 we plot OSNR versus P_{ch} for multiple values of N_s . The figure shows that OSNR keeps increasing till a max point and then starts decreasing. $P_{ch,opt}$ is shown to be independent of N_s . In [52], it is calculated as follows:

$$P_{ch,opt} = \sqrt[3]{\frac{P_{ASE}}{2\eta}} \quad (3.32)$$

This equation shows that $P_{ch,opt}$ is independent of the modulation format and mainly depends on the fiber type, span length, symbol rate (and consequently the channel's bandwidth) and the number of channels in the links as shown in eq. 3.25. All these parameters have constant values in this work unless the number of channels in the link which varies during network operation time.

Hence, to understand the effect of N_{ch} , we plot in Fig. 3.7, OSNR versus P_{ch} for $N_s=25$ spans and multiple number of channels N_{ch} . We have observed the same non-linear attitude as Fig.3.6 with one main difference: $P_{ch,opt}$ changes as the number of channels in the link changes. Therefore, this will make it impossible to decide $P_{ch,opt}$ especially since the number of lightpaths in the link is variable. Moreover, since establishing a new lightpath will degrade the performance of the already established lightpaths, therefore, to guarantee stable performance in the system, we will use the worst-case assumption where we assume that the link is fully loaded and thus, any change in the number of channels is already considered and will not affect its performance. It's true that this is a pessimistic assumption, however, it will guarantee stability. Therefore, P_{ch} is fixed to the $P_{ch,opt}$ at $N_{ch} = 80$.

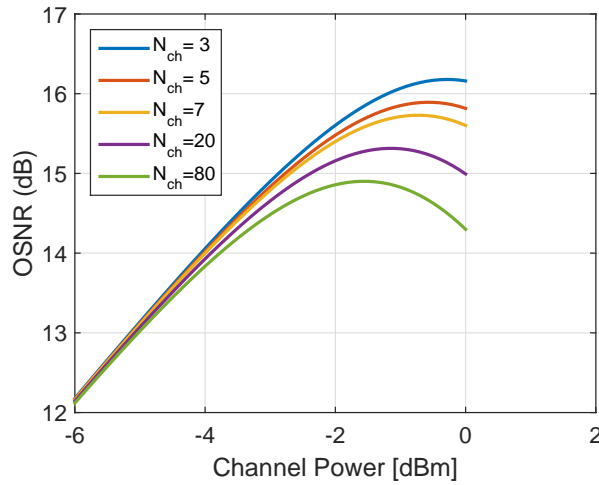


Figure 3.7: OSNR vs P_{ch} for different N_{ch}

3.5 Conclusion

In this chapter we have defined two different transmission layer models: 1) the mixed-line-rate (MLR) model and 2) the Gaussian-noise (GN) model. In the first part, the 100 Gb/s PM-QPSK based on coherent detection, co-exists with the 10 Gb/s OOK based on direct detection and where dispersion is compensated using dispersion-compensating-fibers. The PM-QPSK lightpath performance is degraded mainly due to XPM impacted by OOK channels.

On the contrary, the model in the second part doesn't include dispersion compensating fibers since we have used elastic transponder without including the 10 Gb/s OOK modulation format, thus, dispersion compensating is done thanks to DSP, using electronic compensation. In this case, performance is degraded due to fiber non-linearity resulted mainly due to FWM and thus, the channels' performance estimation is done using the GN-model.

Chapter 4

Simulation Results: Offline Traffic assumption

4.1 Introduction

Satisfying the wavelength-continuity constraint (WCC) becomes harder as demands' path lengths increase, therefore, enabling wavelength conversions enhances network blocking performance through releasing this constraint which increases the capability of the network to serve the demands with longer source (s) to destination (d) paths. However, modulation formats suffer from a trade-off between their transmission reach and their capacity since the higher the capacity, the lower the transmission reach. Thus, as the path length of the demand increases, the probability of using higher-order modulation formats decreases. Hence, to increase networks spectral efficiency and reduce latency, the network is required to route demands over the shortest paths possible. Thus, it increases the allocation of higher-level modulation formats.

Knowing the traffic demands in advance gives an advantage of deciding which traffic to be served first. Authors in [32] show the importance of TSO in wavelength continuous networks which affects the capability of the network to use higher order modulation formats. Thus, in this chapter we study the impact of TSOs on wavelength convertible networks and on the gain obtained of using wavelength converters. Hence, we will use two different TSOs based on demands' traffic volume and demands' shortest-path physical length. The routing algorithm used is the FAR algorithm, the wavelength assignment is the FF and the traffic matrix is based on realistic data [66] which shows that the traffic distribution follows a LogNormal rule.

Network design is done in two stages. First, the design phase or static-RWA, where traffic are known beforehand, and second, the operational phase or dynamic-RWA, where

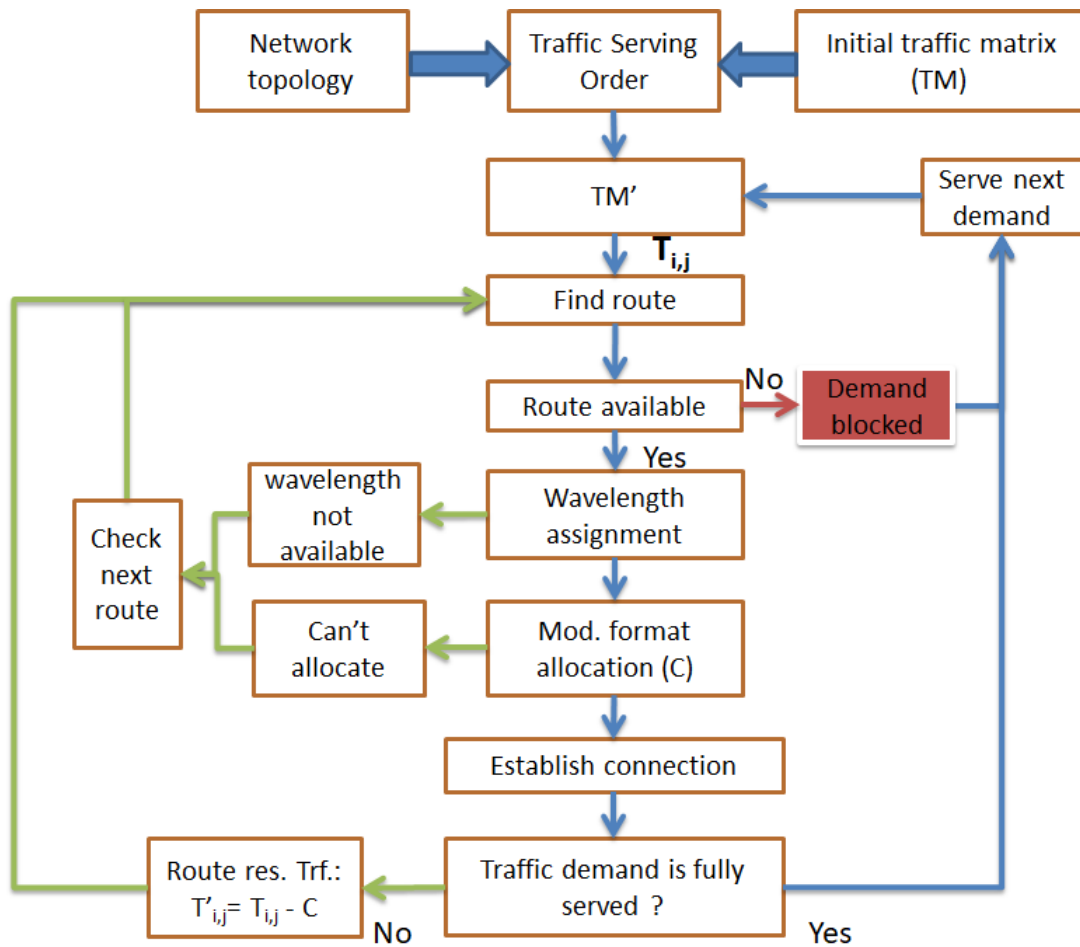


Figure 4.1: Heuristic skeleton

traffic demands arrive sequentially and stay some determined time in the network and leave.

The online design will be detailed in Ch. 5, while the offline network design is studied in this chapter. It is structured as follows: Sec. 4.2 presents the physical and network model, in addition to the simulation and performance parameters. Afterwards, simulation results and their analysis are shown in Sec. 4.3. Finally, Sec. 4.4, concludes this chapter.

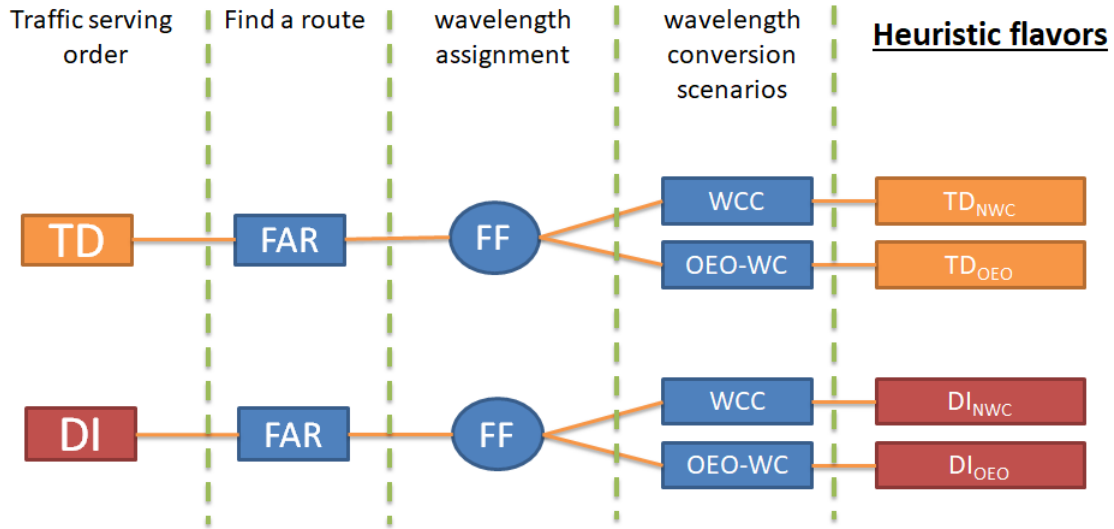


Figure 4.2: Different candidates of the heuristic used.

4.2 Network Model

Static-RWA is considered as an ILP problem which is classified as NP-complete problem (defined in Sec. 2.2.1). Therefore, for real-sized networks, one often has to use a heuristic algorithm to find a sub-optimal solution in reasonable time. The heuristic used in this chapter, to serve the set of traffic demands of the traffic matrix, follows the steps shown in Fig. 4.1. They are explained as follows:

1. On a given physical topology and traffic matrix, the heuristic iteratively satisfies the traffic demands following one of the following TSOs:
 - I Traffic decreasing (TD):
The set of demands are ordered according to their requested bit-rate in the decreasing order and thus, demands are served from the highest to the lowest.
 - II Distance increasing (DI):
The set of demands are ordered according to the physical length of their shortest-path from the lowest to the highest and thus, the heuristic starts by serving the demand whose shortest-path has the shortest physical route length.
2. When the TSO algorithm chooses the demand to be served, $T_{i,j}$ the heuristic finds a route from the set of routes available between source s and destination d using FAR routing algorithms (defined in Sec. 2.2.2.1).

3. Afterwards, to allocate wavelengths, the FF algorithm (explained in Sec. 2.2.2.2) is used. However, based on the type of wavelength converter used, we have the following scenarios:
 - i If wavelength conversions are not allowed, the only constraint is the WCC. Therefore, this scenario is referred to by DI_{NWC} or TD_{NWC} if DI or TD are used, respectively.
 - ii On the other hand, if wavelength conversions are allowed therefore, WCC is released and conversion is done by OEO-WCs where the lightpath's QoT is not affected due to the regeneration. Thus, FF allocates the first available wavelength on each link. These scenario are referred by DI_{OEO} or TD_{OEO} if DI or TD are used respectively.

In case the wavelength assignment algorithm cannot find a solution in the current path, the heuristic goes back to step (2) to check resources in the next path available, based on the routing algorithm used. However, if there are no more paths available, the demand is blocked.

4. When the wavelength assignment algorithm finds a solution, the heuristic calculates the lightpath's $OSNR_{Rx}$ expected at the receiver, and allocates the highest possible modulation format. The modulation formats used in this work are the 100 Gb/s PM-QPSK and 200 Gb/s 16-QAM where their sensitivity is based on a real transponder used in Orange core network scenario [8, 67]. Therefore, if $OSNR_{Rx}$ doesn't satisfy the minimum required sensitivity of the lowest possible modulation format, PM-QPSK, the heuristic goes back to step (2) to check the next path. If there is no more paths available, the demand is blocked.
5. When the modulation format is chosen, if its capacity (C) is higher or equal to the demand's requested bit-rate, then the demand is routed using a single channel. Otherwise, the heuristic goes back to step (2) to serve the demand's residual traffic $T_{i,j} = T_{i,j} - C$ which could be served on different route.

In order to summarize, all the possible heuristic candidates are displayed in Fig. 4.2.

4.2.1 Simulation Parameters

To run the simulations, which are carried in the open-source network planner Net2Plan [68], there are different parameters to be configured:

Average traffic per demand (ATD)

The traffic matrix provides a critical input to research efforts related to performance assessment. Most research studies conducted on these topics make use of

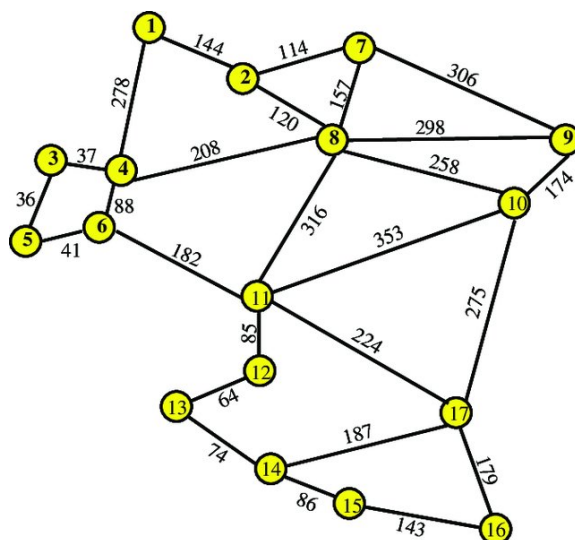


Figure 4.3: 17-Node German network topology.

synthetically generated traffic matrices to evaluate the resulting performance of the scheme being designed. Because almost no data has been published on actual traffic matrices, researchers have had to resort to arbitrary assumptions, some of which can be quite unrealistic. In [66], authors provide some initial solutions for generating synthetic traffic matrices. Their solutions are based on two datasets, one collected from Sprint’s European backbone and one collected from the Abilene’s network; their goal is to determine which probability distribution and corresponding parameters are suitable to be used as random number generators to populate a static traffic matrix. They conclude that, in order to populate a static traffic matrix, a LogNormal distribution must be used. Based on this study, we generate for this work a traffic matrix that has a LogNormal distribution. We vary the average the average traffic per demand (ATD) from 320 Gb/s to 560 Gb/s leading to a total traffic load varying from 80 Tb/s to 160 Tb/s.

Number of wavelengths/fiber (ω)

ω is the available number of wavelengths per fiber which is set to $\omega = 80$.

Alternative paths (κ)

κ is the max number of alternative paths between s and d of each traffic demand. For this chapter, we fix it to $\kappa = 6$.

Physical topology

The physical topology used for these simulations is the 17-Node German topology [8] shown in Fig.4.3, it is characterized as follows: number of nodes is 17, average link length is 170 km and average node degree is 3.05.

4.2.2 Performance Parameters

To compare the quality of service resulted from using the above heuristic candidates, we use the following performance parameters:

Blocked traffic percentage (BTP)

In order to understand how much each heuristic candidate can serve traffic volume, we use the percentage of blocked traffic calculated as follows:

$$BTP = 100 \cdot \frac{\sum_i \sum_j T_{i,j,blocked}}{\sum_i \sum_j T_{i,j,requested}} \quad (4.1)$$

where $T_{i,j, requested}$ and $T_{i,j, blocked}$ are the requested bit-rate to be served and the blocked bit-rate of the traffic demand from i to j , respectively.

Fiber utilized percentage (FUP)

Gives information about the efficiency of using the network spectral resources by the heuristic and its calculated as follows:

$$FUP = 100 \cdot \frac{\sum_1^L NWU_m}{L \cdot \omega} \quad (4.2)$$

where NWU_m is the number of wavelengths used in the fiber m and L is the total number of links in the topology. It is important to note that in order to compare the resulting FUPs of two heuristics, they are supposed to have the same BTP performance and thus, the heuristic that gives a lower FUP among the two is more efficient in terms of spectrum usage than the other heuristic and this is important because operators aim to minimize their use of the available spectrum which increases the probability for future demands to be accepted.

Modulation formats distribution

A demand may be routed over a long path that may not enable the lightpath to be allocated a higher order modulation format. Thus, the allocated format's capacity may be less than the traffic demand required bit-rate to be served, hence, resulting in either blocking some of the traffic or using multiple lightpaths to serve a demand. Therefore, to understand which heuristic favors more the higher order modulation format, the distribution of lightpaths are plotted.

We note that each result is the average of 10 simulations ran for 10 different traffic matrices based on 10 seeds.

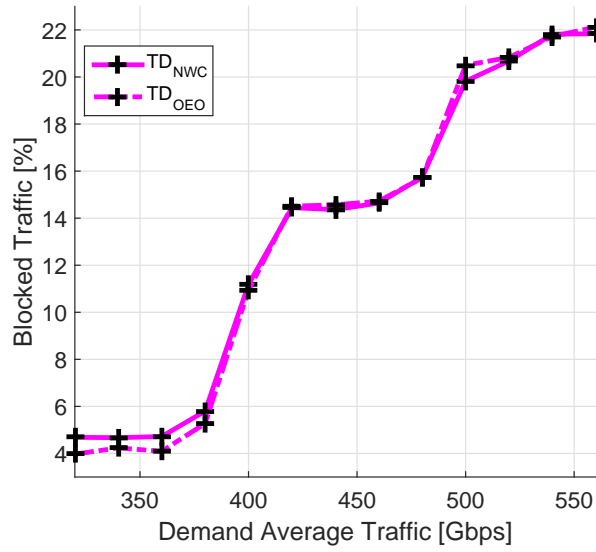


Figure 4.4: BTP vs. ATD using TD-based heuristics.

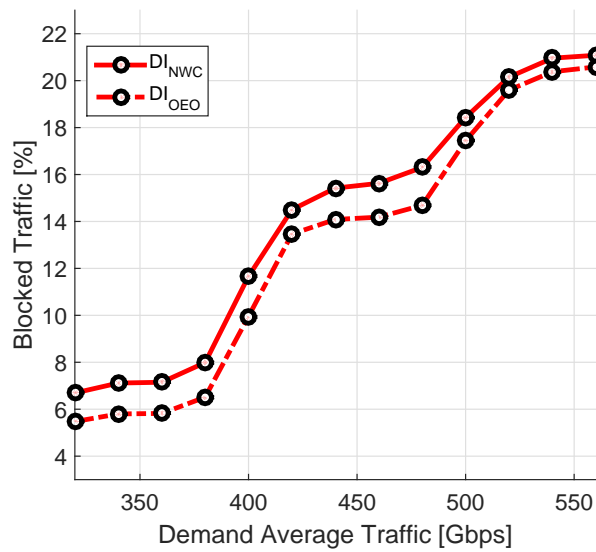


Figure 4.5: BTP vs. ATD using DI-based heuristics.

4.3 Simulation Results

To facilitate results explanations, we will divide them into two sub-sections: in the first one, we compare the gain of using wavelength converters for each TSO separately; in the second sub-section, we compare the performance of TD to that of DI in wavelength

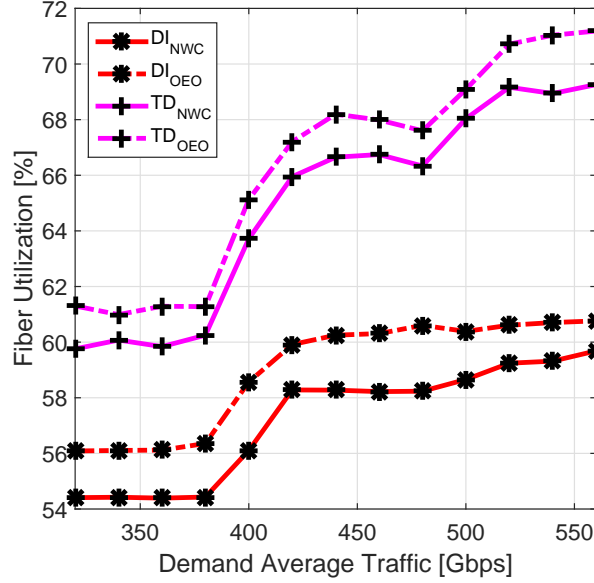


Figure 4.6: FUP vs. ATD using different heuristic candidate.

continuous networks and in wavelength convertible networks.

4.3.1 Sensitivity Of The Gain Of Using Wavelength Converters to TSO

Fig. 4.4 shows the resulting BTP performance of using TD_{OEO} and TD_{NWC} heuristics and Fig. 4.5 shows the resulting BTP performance of using DI_{OEO} and DI_{NWC} heuristics. For $ATD \leq 380$ Gb/s, the BTP gain of using wavelength converters for the case of DI is higher compared to the case of TD. As ATD increases beyond 380 Gb/s, the gain decreases for the case of DI, while it disappears for the case of TD. This decrease in wavelength converters' gain is normal due to the increase in network's congestion with ATD (explained in Sec. 2.3.2). To understand the different gain performance between the two TSOs, we use the FUP and the modulations formats distribution:

The FUP results for all the heuristic candidates are displayed in Fig. 4.6, they are commented as follows. For the case of DI, the FUP ranges between 54.5 to 56 % for $ATD \leq 380$ Gb/s and 56 to 61 % for $ATD \geq 380$ Gb/s, which means that FUP increases by 10 % between the two traffic regimes. On the other hand, for the case of TD, the FUP ranges between 60 to 62 % for $ATD \leq 380$ Gb/s and 62 to 71 % at for $ATD \geq 380$ Gb/s which means that FUP increases by 20 % between the two traffic regimes. Therefore, the increasing slope of FUP for the case of TD is much higher than the case of DI. Hence, as ATD increases, TD results in more congestion compared to DI and this explains why for the case of TD, wavelength converters' gain disappeared faster than

the case of DI.

For deeper analysis, to demonstrate how using wavelength converters affects the routing of demands, modulation formats distributions are plotted in Figs. 4.7 and 4.8 which display the number of lightpaths using 200 Gb/s 16-QAM and 100 Gb/s PM-QPSK resulted of all the heuristics, respectively. The results show that enabling wavelength conversion:

1. doesn't affect the number of lightpaths using 16-QAM for DI (Fig. 4.7);
2. decreases the number of lightpaths using 16-QAM for TD (Fig. 4.7);
3. increases the number of lightpaths using PM-QPSK for TD and DI (Fig. 4.8).

Before analyzing these results, we need to recall two points: i)the modulation format allocation algorithm (explained in Sec. 4.2) allocates the highest possible modulation formats, which means that it is independent of the traffic demand's bit-rate and it depends only on the length of the route. ii)DI serves first the demands whose shortest-path has the shortest physical route lengths. Thus, demands which are allocated 16-QAM modulation format are served first while demands which are allocated PM-QPSK modulation format are served afterwards. Moreover, the first served demands need less wavelength conversions due to short-length nature of demands and due to the very low congestion. Afterwards, as the heuristic starts serving longer demands and the network is more congested (due to the earlier served demands), the need to wavelength conversions increases. Consequently, when DI is used in wavelength convertible networks, wavelength converters are mainly used by lightpaths allocated PM-QPSK, rather than 16-QAM. That's why, we don't see any change in the number of lightpaths using 16-QAM(Fig. 4.7). On the other hand, TD's policy does not give priority to the shortest routes demands, thus, enabling wavelength conversion increases the opportunities of longer routes demands to be served and increases the number of lightpaths using PM-QPSK (Fig. 4.8) and consequently increases network congestion. Therefore, it decreases the probability to serve the short routes demands which consequently decreases the number of lighpaths using 16-QAM in the TD_{OEO} compared to the TD_{NWC} .

4.3.2 TD vs DI in Wavelength Continuous and Wavelength Convertible Networks

In this section TD and DI are compared in two scenarios of wavelength conversion: in the first one, wavelength conversions are not allowed, thus, Fig. 4.9 shows the resulting BTP of using TD_{NWC} and DI_{NWC} heuristics. On the other hand, wavelength conversions are allowed using OEO-WCs, thus, Fig. 4.10 shows the resulting BTP of using TD_{OEO} and DI_{OEO} heuristics. To simplify the analysis, the comparison of TD to DI is divided into three traffic regimes:

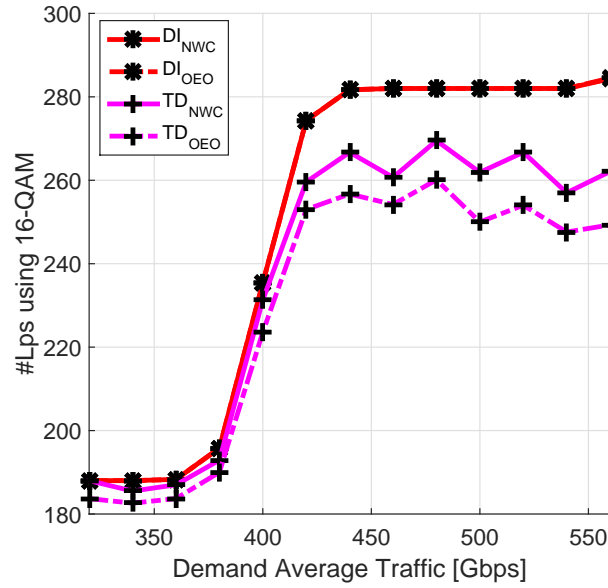


Figure 4.7: No. lihtpaths using 16-QAM vs. ATD using different heuristic candidates.

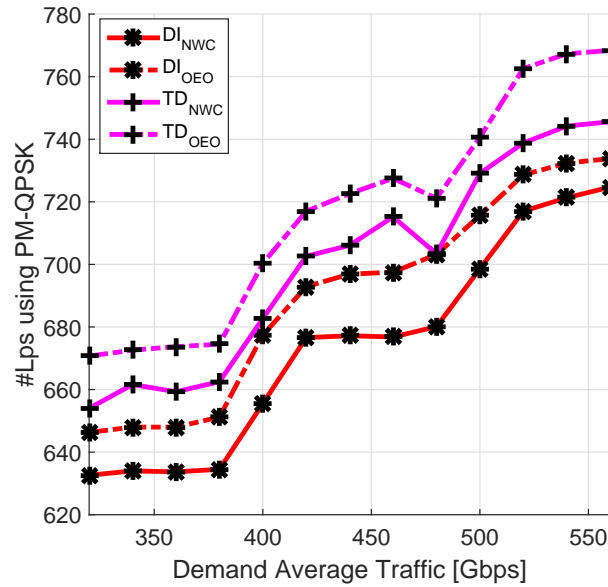


Figure 4.8: No. lihtpaths using PM-QPSK vs. ATD using different heuristic candidates.

1. Lower traffic regime, $ATD \leq 380$ Gb/s:
 TD outperforms DI in terms of the BTP for wavelength convertible network (Fig. 4.9) and wavelength continuous network (Fig. 4.10).

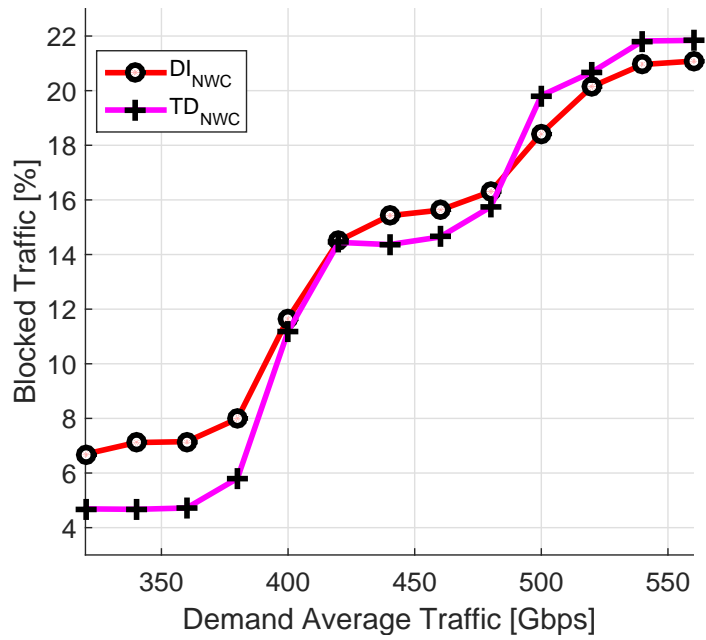


Figure 4.9: BTP vs. ATD for TD vs DI in wavelength-continuous networks.

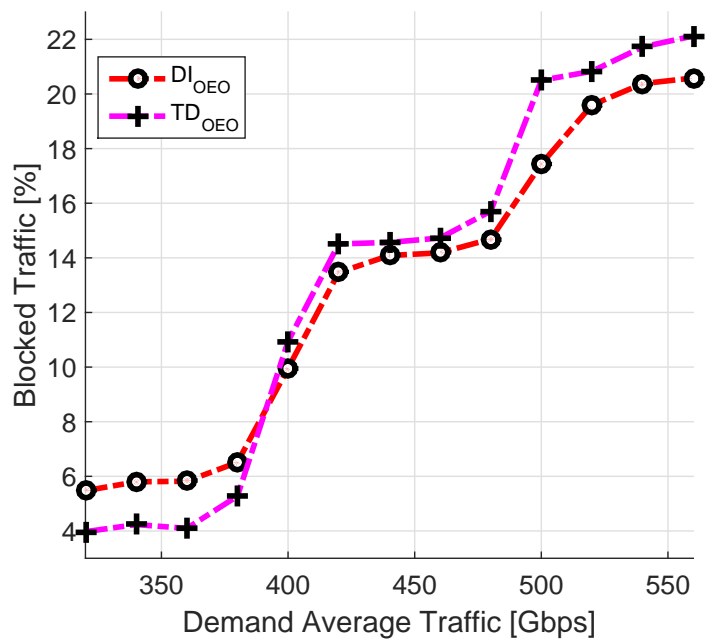


Figure 4.10: BTP vs. ATD for TD vs DI in wavelength-convertible networks.

2. Middle traffic regime, $380 \text{ Gb/s} \leq \text{ATD} \leq 480 \text{ Gb/s}$:

In wavelength continuous network, TD_{NWC} keeps in outperforming DI_{NWC} in terms of the BTP (Fig. 4.9). However, for wavelength convertible network DI_{OEO} starts outperforming TD_{OEO} in terms of the BTP (Fig. 4.10).

3. Higher traffic regime, $\text{ATD} \geq 480 \text{ Gb/s}$:

In this regime, it is totally opposite to the lower traffic regime, DI outperforms TD in terms of the BTP for wavelength convertible network (Fig. 4.10) and wavelength continuous network (Fig. 4.9).

To understand this interchanging of the hierarchies between TD and DI in different traffic regimes, we need to visit the modulation formats distribution results: in the lower traffic regime, the number of lightpaths using 16-QAM resulted of TD heuristic (with and without wavelength converter) is slightly lower than the case of DI (Fig. 4.7). Thus, TD (TD_{OEO} or TD_{NWC}) allocates almost the same number of 16-QAM as DI, which means that at the lower traffic regime with low congestion, not giving the priority to the demands whose shortest-paths have the shortest physical routes doesn't affect the number of 16-QAM allocated up to $\text{ATD} = 380 \text{ Gb/s}$ or 480 Gb/s . Moreover, TD (TD_{OEO} or TD_{NWC}) allocates higher number of lightpaths using PM-QPSK than DI (Fig. 4.8), therefore, it results by TD to outperform DI in terms of BTP in the lower traffic regime (Figs. 4.9 and 4.10).

As ATD increases, DI starts to outperform TD in the middle traffic regime ($\text{ATD} > 380 \text{ Gb/s}$) and higher traffic regime ($\text{ATD} > 480 \text{ Gb/s}$) for wavelength convertible networks and wavelength continuous networks respectively. On the one hand, the reason of this interchange is that at higher congestion levels, DI has higher ability to favor more lightpaths using 16-QAM compared to TD and thus, it serves more traffic. Moreover, even though TD favors higher number of lightpaths using PM-QPSK than DI (Fig. 4.8) but the impact of 16-QAM on performance is higher. On the other hand, the interchange ATD point is different between wavelength convertible network and wavelength continuous network since: enabling wavelength conversion decreases the ability of TD to favor 16-QAM, thus, it explains why DI starts outperforming TD at lower ATD in case of wavelength convertible networks than the case of wavelength continuous networks.

4.4 Conclusion

In this chapter, we have studied the dependence of the gain obtained from using wavelength converters in multi-rate optical network on the TSOs. Therefore, we have designed the network assuming static traffic assumption where the traffic matrix is based on realistic data that has LogNormal distribution. The heuristic algorithm used for solving the RWA problem is based on FAR routing algorithm and FF wavelength allocation algorithm. Moreover, the modulation format allocation algorithm allocates the highest

possible among the modulation format used which are the PM-QPSK 100 Gb/s and 16-QAM 200 Gb/s. Serving the traffic demands was done using two TSOs: TD, which orders the connection demands according to their requested bit-rate, and serve first the demand that requires the highest bit-rate. The second TSO is DI, which orders the connection demands according to the physical length of their shortest-path, and serves first the demand whose shortest-path utilizes the lowest physical route length.

The obtained results show that the gain of using wavelength converters when DI is used, is higher compared to the case of TD. Moreover, the gain in general decreases with ATD but it disappears in the case of TD for $ATD > 380$ Gb/s. On the other hand, comparing TD to DI we conclude the follows results: TD outperforms DI for $ATD < 380$ Gb/s in wavelength convertible networks, and $ATD < 480$ Gb/s in wavelength continuous network. As ATD increases beyond these two points, DI start outperforming TD due to the high congestion resulted by TD which favors less number of lightpaths using 16-QAM compared to DI especially in the wavelength convertible networks and that is why we see that DI started outperforming TD at lower ATD value in wavelength convertible networks than in the case of wavelength continuous networks.

Finally, we note that in this chapter, the wavelength converters is based on OEO-WCs and thus, we didn't consider AO-WCs which will be considered in the next chapter to study if it can replace OEO-WCs in the network operational phase.

Chapter 5

Simulation Results: Online Traffic assumption

5.1 Introduction

After designing the network in the static phase in Ch. 4, and considering the effect of TSO on network gain from using wavelength converters, in this chapter, the network is designed assuming the dynamic traffic assumption. The network model is implemented by discrete-event network simulator where each event occurs at a particular instant in time as shown in Fig.5.1 which displays two types of event: 1) traffic demands arrive the system sequentially following Poisson distribution with average arrival rate per unit time λ . If the demand is served, it occupies resources for a period of time called the holding or service time which is assumed to be uniformly distributed between 0 and 1. 2) After this period, the occupied resources are released, which is called the departure event. On the other hand, if the network can't serve the demand, it is blocked. The amount of blocked demands, in addition to other performance parameters, decide the network quality of service (QoS) which is improved using wavelength converters. Therefore, we need to analyze network performance using AO-WCs and whether they can replace OEO-WCs.

In this chapter, a comparison between AO-WCs' and OEO-WCs' contribution to optical networks performance is done using FAR and LLR routing algorithms (defined in Sec. 2.2.2.1), due to their advantage on improving wavelength conversion contribution in optical networks (as explained in Sec. 2.3.2), and the first-fit (FF) wavelength assignment algorithm is used due to its low complexity (detailed in Sec. 2.2.2.2). Additionally, another wavelength assignment that considers the number of conversions per lightpath is proposed. The heuristics used are introduced in Sec. 5.2. Afterwards, these heuristics will be applied to a real physical topology and the corresponding results are presented in Secs. 5.3 and 5.4.

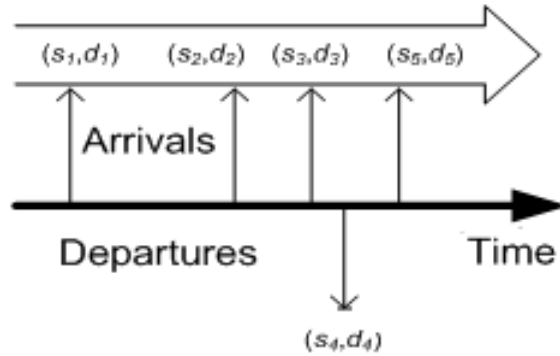


Figure 5.1: Discrete events: arrival and departures.

5.2 Routing, Modulation Format and Wavelength Allocation Algorithms

When a traffic demand arrives to the network, it served using the following heuristic algorithm which has different flavors that are shown afterwards.

5.2.1 Heuristic algorithm

For each demand, the route, modulation format and wavelength are decided using the following heuristic:

1. The heuristic chooses a route with available wavelength resources from the set of routes between source s and destination d using one of the following options of algorithms (defined in Sec.2.2.2.1):
 - I FAR routing algorithm.
 - II LLR routing algorithm.
2. Afterwards, to allocate wavelengths, there two categories of algorithms and for each category there are different possibilities depending on the wavelength conversion scenario. If wavelength conversion is not allowed, the only constraint is the WCC. On the other hand, if conversion is allowed therefore, the WCC is released and conversion is done either by OEO-WCs or AO-WCs: If OEO-WCs are used, the lightpath QoT is not affected due to the regeneration and thus, there is no limitations on conversion. However, if AO-WCs are used, there are limitations on the number of conversions and the conversion range for a channel. Hence, wavelength assignment scenarios are as follows:

A First-fit algorithm (FF):

In this first category, the FF algorithm (explained in Sec.2.2.2.2) is used, thus, based on the type of wavelength converter used, we have the following scenarios:

- i If wavelength converters are not enabled, the only constraint to be satisfied is the WCC. This scenario is referred by FF_{NWC} .
- ii If OEO-WC is used, FF allocates the first available wavelength on each link. This scenario is referred by FF_{OEO} .
- iii If AO-WCs are used, This scenario is referred by FF_{AO} and it works as follows: in every path, if wavelength conversions are enabled, there are a lot of combinations of wavelengths that could be chosen. For example, if the route has m links and the number of wavelengths on each fiber is n , therefore, we have n^m possible combinations of wavelengths that could be chosen. Hence, FF_{AO} allocates the first set of wavelengths that satisfies AO-WCs' limitations.

B Minimum-conversion (MC):

In this category, the MC algorithm is used which is defined as follows. In every path, if wavelength conversions are enabled, there are a lot of combinations of wavelengths that could be chosen. For example, if the route has m links and the number of wavelengths on each fiber is n , therefore, we have n^m possible combinations of wavelengths that could be chosen. Hence, the MC algorithm chooses the combination that uses the least number of conversions among all the combinations available. Compared to the FF algorithm, MC has much higher complexity which increases exponentially with the number of links in the route and number of wavelengths per fiber, however, it aims to decrease the number of wavelength conversions. Hence, based on the type of wavelength converters used, we have the following scenarios:

- i If wavelength converters are not enabled, MC works as FF_{NWC} .
- ii If OEO-WCs are used, this scenario is referred by MC_{OEO} , it aims to find solution that minimizes the number of conversions used and consequently, the energy consumption resulting from OEO-conversions.
- iii If AO-WCs are used, MC chooses a combination of wavelength that not only requires the minimum number of conversions per channel, but that satisfies AO-WCs' limitations also. This scenario is referred to by MC_{AO}

In case the wavelength assignment algorithm cannot satisfy the conditions (WCC or AO-WCs' limitations) in the current path, the heuristic goes back to step (1) to check resources in the next path available, based on the routing algorithm used. If there are no more paths available, the demand is blocked.

3. In case the wavelength assignment algorithm finds a solution that satisfies the required conditions, the heuristic calculates the lightpath's OSNR_{Rx} expected at the receiver, and allocates the highest possible format. The modulation formats used in this work are the PM-QPSK 100 Gb/s and 16-QAM 200 Gb/s where their sensitivity is based on real transponders used in Orange core network scenario [8, 67]. Therefore, if OSNR_{Rx} doesn't satisfy the sensitivity of the PM-QPSK, the heuristic checks the next path. If there are no more paths available, the demand is blocked.

5.2.2 Heuristics Flavors

In the previous section, there are different possible combinations that could be obtained using 2 different routing algorithms and 5 different wavelength assignment algorithms which result in 10 flavors of the heuristic used. Thus, in order to summarize all possible heuristic flavors are displayed in Fig. 5.2.

However, we note that for any heuristic that enables wavelength conversion, we try to serve the demand first without wavelength converters in order to guarantee that all the alternative paths can't satisfy the WCC, then, if the demand can't be served, we use the heuristic required to satisfy the demand. For instance, if the heuristic applied is FAR-MC_{AO}, we try to serve the demand using FAR-FF_{NWC}, where wavelength conversion are not allowed and thus, if all the paths can't satisfy the demand, we use FAR-MC_{AO}. The same strategy is applied if FAR-FF_{OEO}, FAR-FF_{AO} and FAR-MC_{OEO} are used. Moreover, if the heuristic applied is LLR-FF_{OEO}, LLR-FF_{AO}, LLR-MC_{OEO} or LLR-MC_{AO}, we try to serve the demand using LLR-FF_{NWC} heuristic flavor first.

The aim of having this variety of flavors is to understand the sensitivity of the network performance gain obtained by using AO-WCs to the routing and wavelength assignment algorithms and other parameters, which are defined in the next section, in order optimize this gain.

5.2.3 Simulation Parameters

Based on the heuristics introduced before, the simulation parameters to be configured are as follows:

Arrival rate (Λ)

Λ is the demands' average arrival rate per unit time to the network. It is, in addition other parameters, the network's load since the higher it is, the more network is congested or loaded.

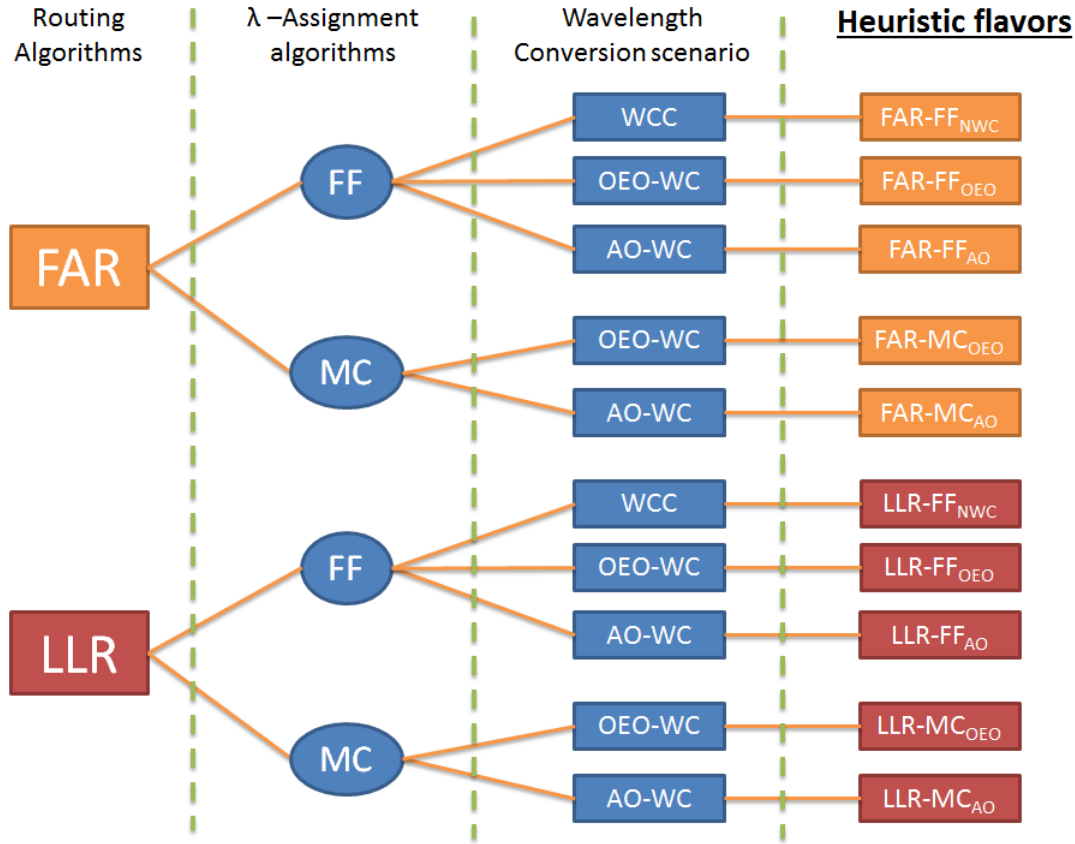


Figure 5.2: Different flavors of the heuristic used.

Number of wavelengths/fiber (ω)

ω is the available number of wavelengths per fiber initially.

Network's load

Network load: as explained in Chapter II, blocking at high network congestion is mainly due to the non-availability of wavelength resources, whereas, at low network congestion, this problem probability is very low, since the blocking is either due to the WCC constraints or not satisfying AO-WCs' limitations and OSNR requirements. Therefore, to monitor the gain of wavelength converter and then understand how this gain is impacted when AO-WCs is used instead of OEO-WC, it's important to work at lower congestion level, which is directly related with Λ and ω : it increases with Λ while it decreases with ω . Hence, to vary network load, we should vary Λ , however, we will fix ω for two reasons: 1)it is usually fixed in network and decided beforehand during the offline phase; 2)increasing ω will increase the complexity of the MC wavelength assignment, therefore, we intend to fix it at $\omega=15$.

Alternative paths (κ)

The routing algorithms used in this thesis are FAR or LLR and in both cases there should be a set of routes between each demand's source and destination, therefore, one of the main simulation parameters is the max number of alternative paths, κ , which is ranged between $\kappa= 1$ to 6.

AO-WCs' cascadability (C)

To consider wavelength converters' limitations, we consider the cascadability (defined in Sec. 2.3.1.2), therefore, the maximum number of cascaded wavelength converters allowed is defined as C.

AO-WCs' tuning range (R)

Another limitation of AO-WCs is the tuning range (defined in Sec. 2.3.1.2), therefore, it is defined as R. For example, if tuning range is set to 250 GHz, which is equivalent to the bandwidth of 5 channels, we will say $R= 5 \times 50$ GHz and in this case, R is 33.3 % of the full range which is 15×50 GHz (15 is the total number of wavelengths per fiber defined above).

Simulation time

The simulations keeps running until a specific number of demands arrived to the network, either served or blocked. This number is set to 10,000 demands.

Buffering time

Generally, in network design, when a demand arrives to the network, if it can't be served, it may be saved in the buffer for a limited buffering time. However, in this work, buffering is not allowed in order to trace the gain of using wavelength converter in a network.

Physical topology

The physical topology used to run simulations is the German topology shown in Fig.4.3, it is characterized as follows [8]: number of nodes is 17, average link length is 170 km and average node degree is 3.05.

5.2.4 Performance Metrics

The network performance is estimated using the following parameters:

Blocking

One of the main targets of network design is to serve the highest possible number of demands for a fixed number of transceivers or wavelengths. In other words, the target is to reach the lowest blocking possible with fixed resources. Therefore, to estimate which wavelength assignment or routing algorithms can better optimize the performance, we use the percentage of the number of demands blocked over the total number of demands required to be served.

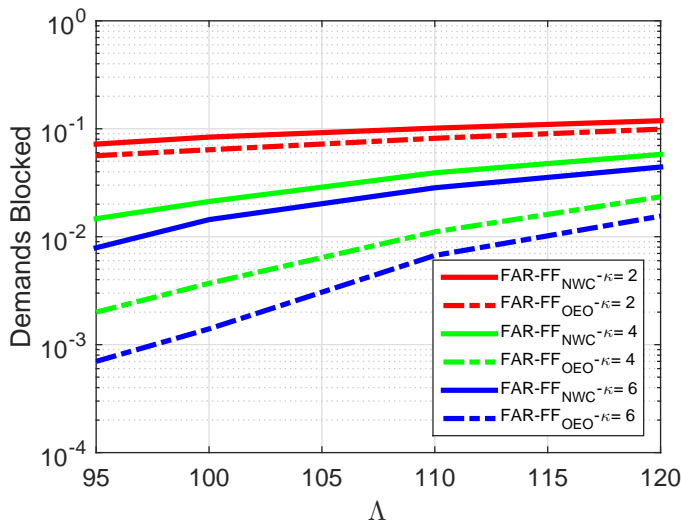


Figure 5.3: Blocking versus arrival rate (Λ) using FAR-FF_{NWC} and FAR-FF_{OEO} heuristics at different κ .

Modulation formats distribution

It is true that serving more demands is the major priority in network design, however, a demand may be routed over a long path that may not enable the use of higher order the modulation format, and thus, the allocated modulation format may have a capacity less than the required traffic volume to be served, hence, resulting in either blocking some of the traffic or using multiple lightpaths if wavelength resources are available. Therefore, to understand which heuristic is favoring more the higher order modulation format, the percentage distribution of lightpaths using the 200 Gb/s 16-QAM, since it is the highest-level format, used by the served demands.

Number of conversions

This performance parameter reflects the cost especially if OEO-WC is used, then it reflects energy consumption. Moreover, at a fixed blocking, the lower the number of conversions, the lower is the need for wavelength converters.

5.3 Simulation Results: The Gain of Using OEO-WCs

In this section we compare wavelength continuous network performance with wavelength convertible network using OEO-WCs and analyze the effect of different parameters such as Λ , κ , the wavelength assignment (FF or MC) and the routing algorithms (FAR or LLR).

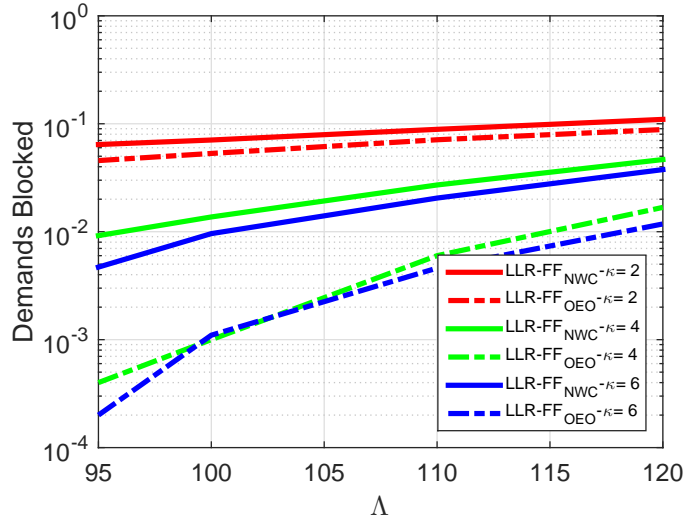


Figure 5.4: Blocking versus arrival rate (Λ) using LLR-FF_{NWC} and LLR-FF_{OEO} heuristics at different κ .

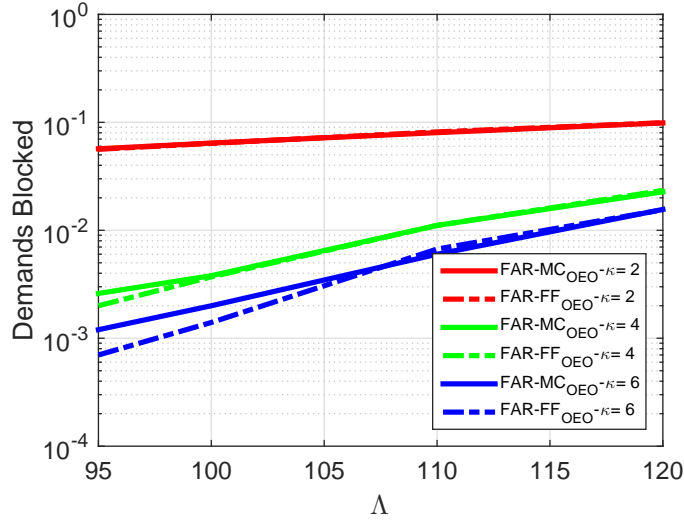


Figure 5.5: Blocking versus arrival rate (Λ) using FAR-FF_{OEO} and FAR-MC_{OEO} heuristics at different κ .

5.3.1 Sensitivity to the Number of Alternative Paths

To understand the effect of κ on OEO-WCs network performance gain, the percentage of blocked demands versus Λ for different κ are plotted as follows: Fig 5.3, where FAR and FF are used, shows the performance of FAR-FF_{NWC} and FAR-FF_{OEO} heuristics. Fig 5.4,

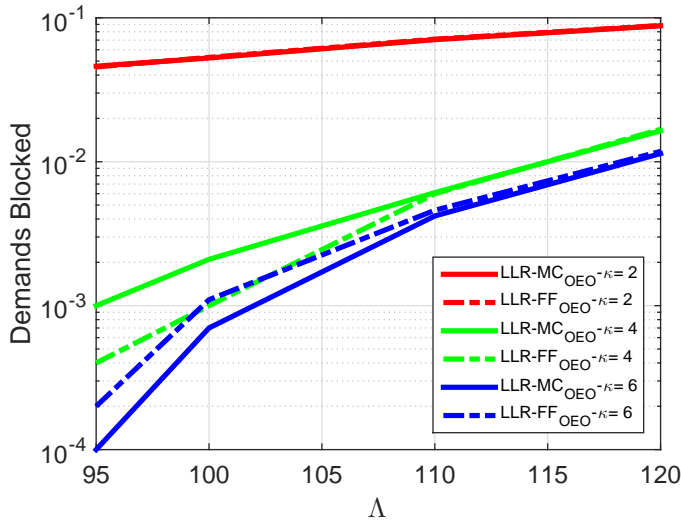


Figure 5.6: Blocking versus arrival rate (Λ) using LLR-FF_{OEO} and LLR-MC_{OEO} heuristics at different κ .

where LLR and FF are used, shows the performance of LLR-FF_{NWC} and LLR-FF_{OEO} heuristics. The same conclusions are made for both figures: 1) the blocking increases with Λ due to the increase in the network load and thus, increase in network congestion which leads to the decrease of the wavelengths resources availability. On the contrary, the blocking at lower load is mainly due to the WCC, therefore, using OEO-WCs significantly improves the performance at lower load comparing to its humble contribution at high congestion. Moreover, 2) this contribution increases with κ since the probability to satisfy WCC decreases with longer routes, therefore, using OEO-WCs increases the probability to route demands over longer paths and consequently, increases OEO-WCs' contribution to network blocking enhancement.

5.3.2 Sensitivity to Wavelength Assignment Algorithms

In the previous section, we have demonstrated the impact of κ using the two different routing algorithms while with just the FF wavelength assignment. Therefore, to understand the impact of MC wavelength assignment, we plot the percentage of blocked demands using FAR-FF_{OEO} and FAR-MC_{OEO} heuristics in Fig. 5.5 and LLR-FF_{OEO} and LLR-MC_{OEO} heuristics in Fig. 5.6. The results show that MC_{OEO} and FF_{OEO} have almost the same blocking performance for the same routing algorithm.

On the other hand, since MC aims to minimize the number of conversions, we plot the it using FAR-FF_{OEO} and FAR-MC_{OEO} heuristics in Fig. 5.7 and using LLR-FF_{OEO} and LLR-MC_{OEO} heuristics in Fig. 5.8. The results show that MC significantly decreases

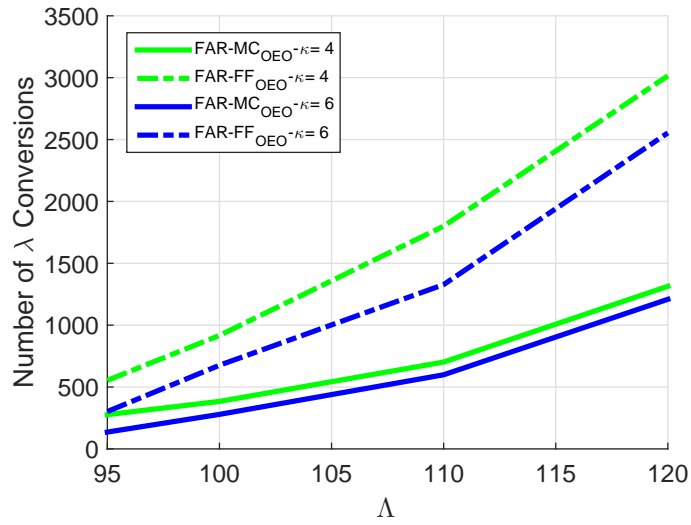


Figure 5.7: Number of conversions vs. arrival rate using FAR-FF_{OEO} and FAR-MC_{OEO} heuristics at different κ .

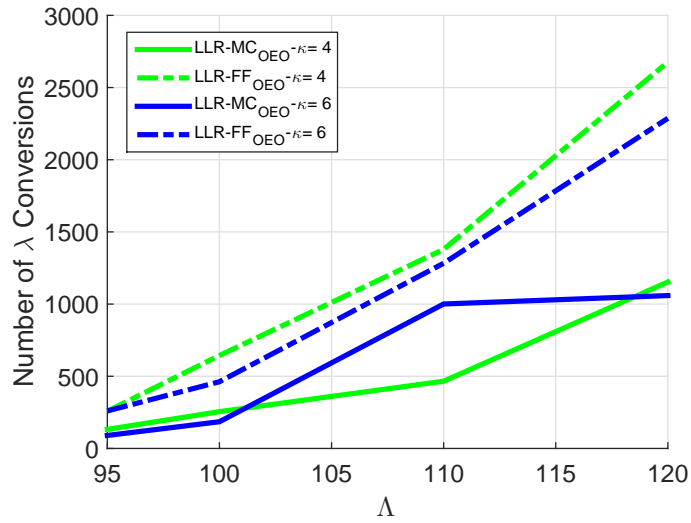


Figure 5.8: Number of conversions vs. arrival rate using LLR-FF_{OEO} and LLR-MC_{OEO} heuristics at different κ .

the number of conversions used with respect to FF especially at high traffic load, or high Λ , where the need for wavelength conversions increases due to congestion and thus, using a simple wavelength assignment that targets only to find wavelengths resources will increase the number of conversions used comparing to MC which economize this need. Moreover, the number of conversions also is impacted by κ since increasing it

will increase the probability of the demands to be routed over alternative paths without using wavelength conversions because the policy is not to use wavelength conversion unless serving the demand failed to satisfy the WCC constraints at the beginning. We note the number of conversions in Figs. 5.7 and 5.8 are plot for $\kappa= 4$ and 6 only since at $\kappa= 2$ we didn't notice any gain for OEO-WCs.

5.3.3 Sensitivity to Routing algorithms

The sensitivity to routing algorithm is studied based on two performance parameters, the blocking ratio and the modulation formats distribution.

Blocking Performance

After understanding the impact of κ and wavelength assignment on OEO-WCs gain, we are left with the routing algorithms effect. Therefore, to compare FAR to LLR in wavelength convertible networks, the percentage of blocked traffic versus Λ for FAR-FF_{OEO} and LLR-FF_{OEO} heuristics are plot in Fig. 5.9 and FAR-MC_{OEO} and LLR-MC_{OEO} heuristics in Fig. 5.10. The plots clearly show that LLR outperforms FAR in both wavelength assignments and this is explained as follows: FAR routes demands over the first available path from shortest to longest, therefore, this policy may lead some physical links to be fully congested and consequently, blocking demands that arrive afterwards. On the contrary, LLR routes demands over the least congested path which distributes traffic between the alternative path and thus, at low load regime, it doesn't allow links to be fully congested which enhances its performance in comparison with FAR. However, this advantage decreases as the traffic increases since network will have to be congested over all its links.

Modulation Format Distribution Performance

On the other hand, since LLR routes the demands without considering the length of the path, thus, it decreases the probability of using higher order modulation formats in comparison to FAR routing algorithm which gives priority to the shortest paths between the source and destination of any demand. Fig. 5.11 shows the percentage of lightpaths using 200 Gb/s 16-QAM versus Λ when FAR-FF_{OEO} and LLR-FF_{OEO} heuristics are used while Fig. 5.12 shows the results when FAR-MC_{OEO} and LLR-MC_{OEO} heuristics are used. The results show that, independent from the wavelength assignment used: at $\kappa= 2$, where the difference between FAR and LLR is very low, the percentage dropped from 44 % (for the FAR case) to 39 % (for the LLR case). Moreover, at $\kappa= 4$ or 6, the percentage dropped from 41 % (for the FAR case) to 33 % (for the LLR case). Hence,

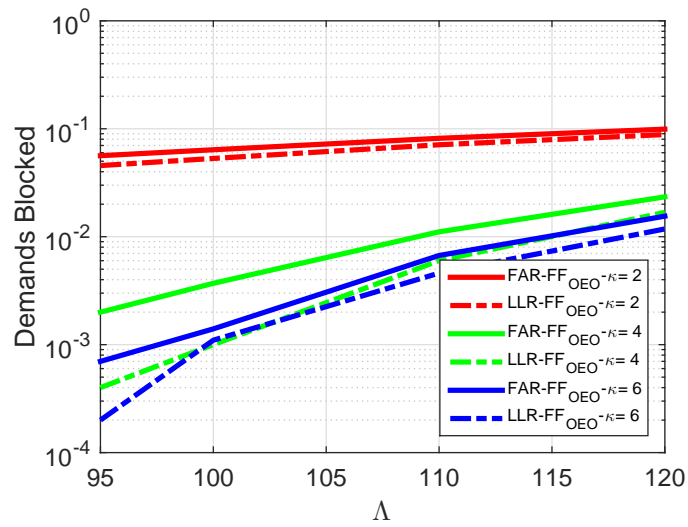


Figure 5.9: Blocking versus arrival rate (Λ) using FAR-FF_{OEO} and LLR-FF_{OEO} heuristics at different κ .

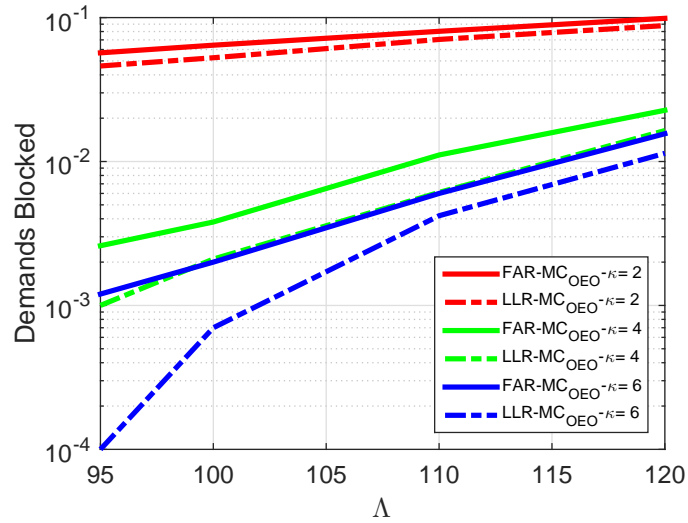


Figure 5.10: Blocking versus arrival rate (Λ) using FAR-MC_{OEO} and LLR-MC_{OEO} heuristics at different κ .

comparing FAR to LLR, there is a trade-off between the blocking performance and the level of the modulation formats used by the lightpaths.

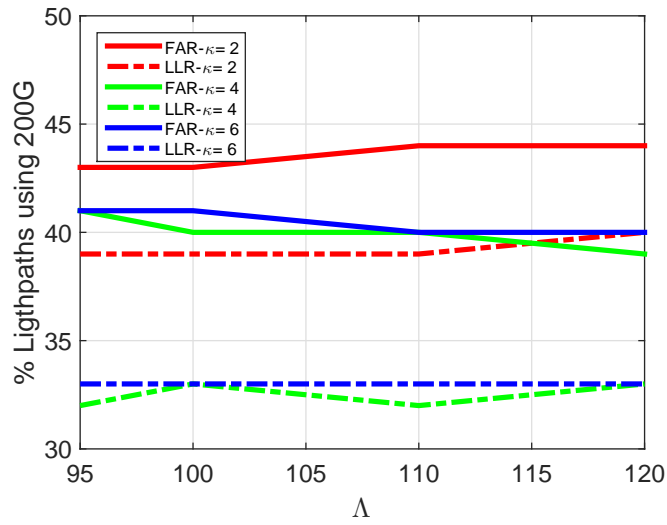


Figure 5.11: % lightpaths using 200 Gb/s vs. Λ in FAR-FF_{OEO} and LLR-FF_{OEO} heuristics at different κ .

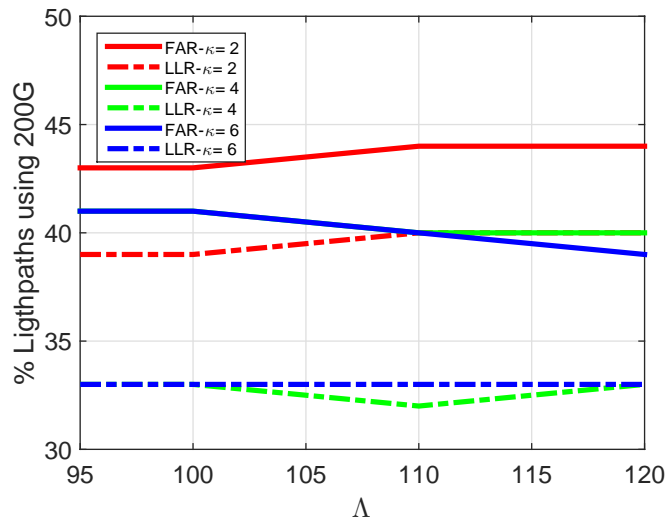


Figure 5.12: % lightpaths using 200 Gb/s vs. Λ in FAR-MC_{OEO} and LLR-MC_{OEO} heuristics at different κ .

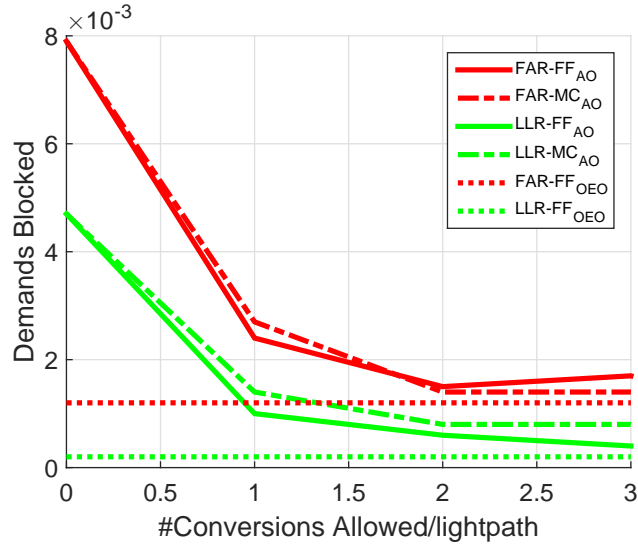


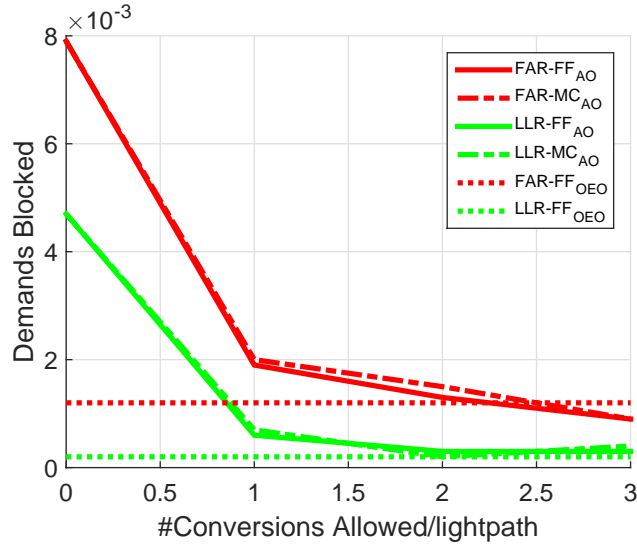
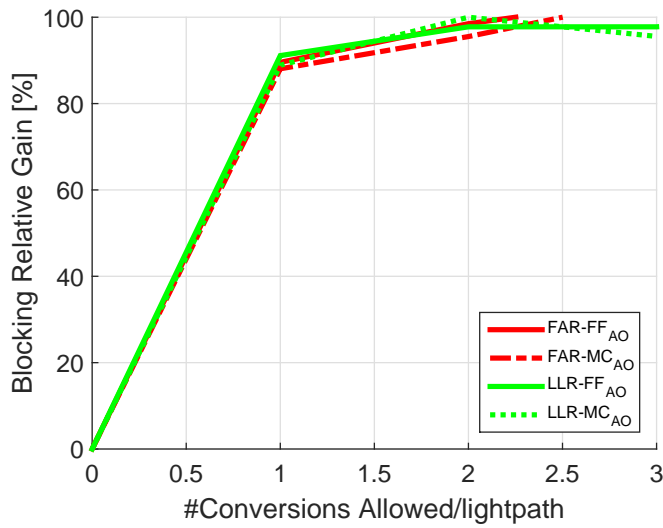
Figure 5.13: % Blocking vs. C at $\Lambda=95$, $R=2 \times 50$ GHz and $\kappa=6$.

5.4 Simulation Results: Network Gain from Using AO-WCs

After demonstrating the impact of each factor on the OEO-WCs' gain in the previous section, we need to know if AO-WCs with their limitations can have the same contribution in enhancing network performance. Therefore, using AO-WCs, we will study the sensitivity of the contribution to the maximum number of conversions allowed per lightpath, C , and converters' maximum conversion range allowed, R . For this issue, we will do the analysis in the zone where the highest gain obtained from using OEO-WCs is observed, thus, the number of alternative paths is fixed to $\kappa=6$, the arrival rate is fixed to $\Lambda=95$, the lowest traffic regime.

The heuristics used here are the ones that consider AO-WCs: $\text{FAR-FF}_{\text{AO}}$, $\text{FAR-MC}_{\text{AO}}$, $\text{LLR-FF}_{\text{AO}}$ and $\text{LLR-MC}_{\text{AO}}$. Their corresponding blocking performance versus C are plot in Figs. 5.13 and 5.14 corresponding to $R=2 \times 50$ GHz (13.3 % of the full range) and $R=4 \times 50$ GHz (26.6 % of the full range), respectively. Moreover, in each figure there are two horizontal dotted lines, which consider the cases where OEO-WCs are used, in red and in green which refer to $\text{FAR-FF}_{\text{OEO}}$ and $\text{LLR-FF}_{\text{OEO}}$ at $\Lambda=95$ and $\kappa=6$. These lines are references to check at what C and R do the AO-WCs give the same performance as OEO-WCs. Looking at the figures, the following conclusions are derived:

In Fig. 5.13, where $R=2 \times 50$ GHz, the blocking performance with AO-WCs cannot reach the blocking performance with OEO-WCs for all the heuristics. However, as R


 Figure 5.14: % Blocking vs. C at $\Lambda=95$, $R=4 \times 50$ GHz and $\kappa=6$.

 Figure 5.15: $Gain_{relative}$ vs. C at $\Lambda=95$, $R=4 \times 50$ GHz and $\kappa=6$.

increases to $R=4 \times 50$ GHz, the blocking performance with AO-WCs reaches the same blocking performance as OEO-WCs, at $C=2$ for the LLR and at $C=3$ for the FAR routing algorithms. This difference in the number of conversions required is due to the difference in congestion between the two routing algorithms and thus, routing the demand in the least-congested path, will decrease its need to undergo conversions comparing to FAR where lightpath is pushed to undergo more conversion to be routed in the first available path.

Furthermore, at $C=1$ and $R=2 \times 50$ GHz (Fig. 5.14), LLR-FF_{OEO} and LLR-MC_{OEO} performances reach the red dotted line, which corresponds to the blocking performance of the network when FAR is used with OEO-WCs. This means that using LLR routing algorithm, with only 1 conversion allowed per lightpath, the blocking performance can reach the same level of using FAR routing algorithm with OEO-WCs. However, we shouldn't ignore that LLR leads to a decrease in the number of lightpaths that use the higher modulation formats 16-QAM 200 Gb/s.

Another interesting point comes out when the relative gain, which is defined as follows, is observed:

$$Gain_{relative} = \frac{Gain_{AO}}{Gain_{OEO}} \quad (5.1)$$

where $Gain_{AO}$ and $Gain_{OEO}$ are the blocking gain of using AO-WCs and OEO-WCs respectively, it is defined as follows:

$$Gain = \frac{Blocking_{NWC}}{Blocking_{WC}} \quad (5.2)$$

where $Blocking_{NWC}$ and $Blocking_{WC}$ are the resulting blocking percentages in wavelength continuous network and wavelength convertible networks respectively. The relative gain for all heuristics are plotted in Fig. 5.15, we notice that it reaches up to 90 % at $C=1$ for all the heuristics. This is very interesting in the case of AO-WCs where the more the lightpath undergoes conversion with AO-WCs, the more the performance is degraded, thus, allowing only 1 conversion per lightpath to reach up to 90 % of what OEO-WCs can achieve, means that AO-WCs can replace OEO-WCs with slight difference in performance at network level.

Moreover, in terms of cost, if the number of conversions per channel is limited to 1, even when OEO-WCs are used, this will significantly decrease energy consumption through decreasing the total number OEO conversions. To clarify this, the number of conversions used in each heuristic versus C , are plotted in in Figs. 5.16 and 5.17 for FAR and LLR routing algorithms, respectively. In each figure, the results shown corresponds to the FF and MC wavelength assignment. Moreover, in each figure there are two horizontal lines corresponding to the cases when no limitation is imposed on number of conversions per lightpath. The results show that limiting the number of conversions per lightpath will dramatically decrease the total number of conversions up to 60 % at $C=1$ in the cases of FAR-FF and LLR-FF while there is no notable change in the cases FAR-MC and LLR-MC. This means that in the cases where the FF wavelength assignment, limiting the number of conversions will decrease the total number of conversions and even make it approximately equal to the case of MC.

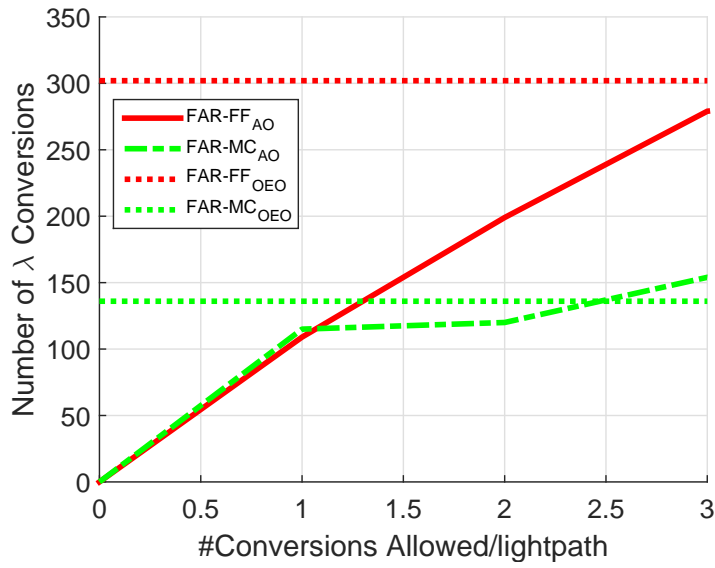


Figure 5.16: Number of conversions vs. C at $\Lambda= 95$, $R= 4 \times 50$ GHz and $\kappa= 6$ using FAR.

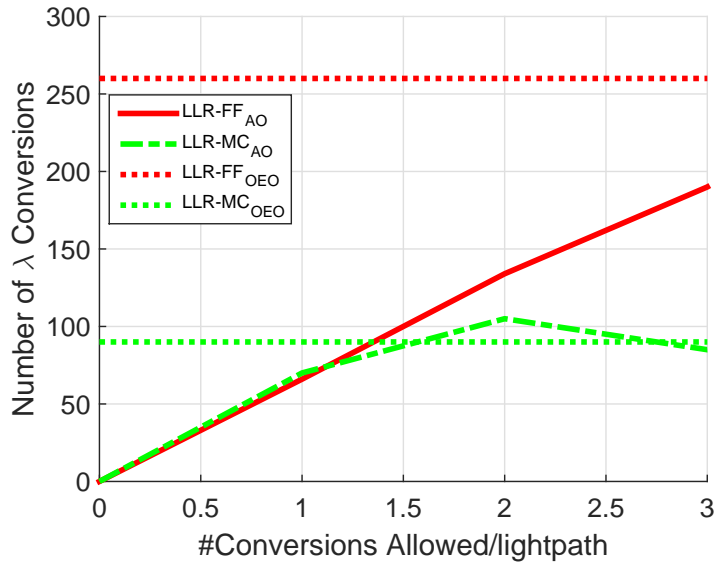


Figure 5.17: Number of conversions vs. C at $\Lambda= 95$, $R= 4 \times 50$ GHz and $\kappa= 6$ using LLR.

5.5 Conclusion

In this chapter we have designed the network assuming dynamic traffic assumption aiming to compare wavelength convertible performance using AO-WCs and OEO-WCs. For the the routing algorithms, we have used FAR and LLR, for the wavelength assignment we have used the FF and we have introduced the minimum number of conversions per lightpath (MC) algorithm. The modulation formats used are 100 Gb/s PM-QPSK and 200 Gb/s 16-QAM and the lightpath is assigned the highest possible formats based on the expected OSNR at the receiver.

The results have shown that AO-WCs of a maximum number of wavelength conversions per lightpath $C= 2$ or 3 for the LLR and FAR routing algorithms, respectively, and a tuning range $R= 4 \times 50$ GHz (less than 30 % of the full spectrum range) achieve the same network blocking performance as OEO-WCs. Moreover, using AO-WCs at $C=1$: 1)FAR and LLR reach 90 % of OEO-WCs' network blocking performance enhancement (independent of the wavelength assignment used) and 2) when FF is used (with LLR or FAR), the number of conversions saved are more than 50 % comparing to the case when OEO-WCs without any limitations. 3)LLR achieved the same blocking performance as FAR with OEO-WCs. However, FAR have shown the ability to favor higher order modulation formats more than LLR.

Finally, In terms of wavelength assignment, FF and MC have shown the same blocking performance however, MC significantly outperforms FF in terms on number of conversion used and this is good when OEO-WCs are used due to the energy MC through decreasing the OEO conversions.

Chapter 6

Conclusions and future work

6.1 Summary and Conclusions

In this work, we have investigated AO-WCs (which are limited in their cascadability, tuning range and they degrade channel's QoT) ability to replace conventional OEO-based wavelength converters (OEO-WCs, which are able to perform wavelength conversion without affecting the quality of the converted channel) and give the same network's blocking performance enhancement in WDM multi-rate all-optical networks.

We have used two different transmission layer models based on two different categories of modulation formats and bit-rates. In the first one, CD is compensated using DCFs in the case of the legacy 10 Gb/s OOK which coexists with the 100 Gb/s PM-QPSK where CD compensation is done electronically. This is known as MLR model where the 10 Gb/s OOK impacts the 100 Gb/s PM-QPSK performance due to XPM. On the other hand, due to the need to move towards using higher-order modulation formats based on elastic transponder, the second transmission model includes modulation formats based on coherent detection and electronic CD compensation which makes no need for DCFs. This is known as uncompensated-transmission.

For the network model, the routing algorithms used are the FAR and LLR due to their importance in optimizing the performance of wavelength-convertible network. Moreover, for the wavelength assignment problem, we have used the FF and MC (find the set of wavelengths that uses the minimum number of conversions in the path) algorithms. Independently of the wavelength assignment algorithms used, the results show:

- LLR outperforms FAR in terms of the ratio of blocked demands, however, it alleviates the capability of the network to use higher-order modulation format since it doesn't consider the length of the route but only its congestion.

- In case of LLR routing algorithm, for a maximum number of wavelength conversion allowed per channel $C= 2$, AO-WCs results the same the performance as OEO-WCs. On the other hand, for FAR routing algorithm, the performance reached the same as OEO-WCs at $C= 3$. The maximum conversion range allowed per channel for both routing algorithms was $R= 4 \times 50$ GHz (less than 30 % of the total spectrum range assumed 15×50 GHz).
- Using LLR routing algorithm, AO-WCs with $R= 4 \times 50$ GHz and $C= 1$ results the same blocking performance as FAR routing algorithm with OEO-WCs.
- Using LLR or FAR routing algorithms, AO-WCs with $R= 4 \times 50$ GHz and $C= 1$, achieve 80 to 90 % of the blocking gain of OEO-WCs.

This means that AO-WCs, with the results shown in literature especially in terms of cascadability, are able to yield the same network performance as OEO-WCs. Moreover, using LLR routing algorithm, in addition to outperforming FAR, show less need number of conversions per lightpath which makes it more suitable to be used in case of AO-WCs. On the other hand, in terms of wavelength assignment, MC reduces significantly the total number of wavelength conversions done compared to FF. This result is good for the case of OEO-WCs since MC reduces energy consumption

The former study has been conducted assuming dynamic traffic assumption, however, in the static phase of the network where traffic are know beforehand, there is an advantage of ordering the demands of the traffic matrix. Therefore, this thesis has also studied the dependence of network's performance enhancement due to OEO-WCs on the TSOs where the traffic are served either in the decreasing order of traffic demands' capacity (TD) or the increasing order of traffic demands' shortest-path (DI). The routing and wavelength assignment algorithms are FAR and FF respectively. Simulation results showed that:

- The gain of wavelength converters using DI is higher compared to TD especially at the higher traffic regime where the gain in the TD case disappears.
- TD outperforms DI in the lower traffic regime, however, as traffic increases, DI outperform TD in the higher traffic regime.
- DI has higher ability to favor higher-order modulation formats compared to TD which affects the results in the higher traffic regime where the need of higher capacity modulation formats is critical.

6.2 Future Research Proposals

While the main objective of this research has been fulfilled, several research opportunities could be derived from the material presented in this thesis. We propose some directions for future research:

- The topology chosen for this work has short average links lengths in order to guarantee that blocking of demands is done either due to lack of wavelength resources or WCC. Hence, another realistic topologies with longer links lengths should be investigated to confirm results obtained in this work.
- The routing algorithms considered are FAR and LLR which weight the paths based either on their length or their congestion level. However, we need to test another routing algorithms which weight the path based on AO-WCs constraints while take the routing decision. For instance, a routing algorithm that routes the demand over the path which needs minimum number of conversion per channel.
- AO-WCs limitations considered in this work were in terms of the maximum tuning range and maximum number of conversions allowed, however, when a channel undergoes a wavelength conversion, its QoT is degraded. Therefore, we need to add an OSNR penalty to have more precise scenarios.
- In this thesis, we have assumed the full wavelength conversion scenario (defined in Sec. 2.3.1.1) to simplify analysis. However, wavelength converters are expensive devices, thus, it is not economically possible to equip all nodes in a WDM network with these devices. Therefore, after our investigations of how to benefit from AO-WCs, we need to consider the wavelength-placement problem which should also take into considerations AO-WCs limitations.

Bibliography

- [1] Lightwave-Staff, *Coherent 400G, edge 100G future growth catalysts: Cignal AI*, July 30, 2018. [Online]. Available: <http://engineering.purdue.edu/~mark/puthesis>
- [2] S. Azodolmolky, M. Klinkowski, E. Marin, D. Careglio, J. S. Pareta, and I. Tomkos, “A survey on physical layer impairments aware routing and wavelength assignment algorithms in optical networks,” *Computer Networks*, vol. 53, no. 7, pp. 926 – 944, May 2009.
- [3] X. Chu, J. Liu, and Z. Zhang, “Analysis of Sparse-Partial Wavelength Conversion in Wavelength-Routed WDM Networks,” in *IEEE INFOCOM*, 2004.
- [4] J. M. Yates, M. P. Rumsewicz, and J. P. R. Lacey, “Wavelength converters in dynamically-reconfigurable WDM networks,” *IEEE Communications Surveys*, vol. 2, no. 2, pp. 2–15, Second Quarter 1999.
- [5] F. Cugini, N. Sambo, N. Andriolli, A. Giorgetti, L. Valcarenghi, P. Castoldi, E. L. Rouzic, and J. Poirrier, “Enhancing gmpls signaling protocol for encompassing quality of transmission (qot) in all-optical networks,” *Journal of Lightwave Technology*, vol. 26, no. 19, pp. 3318 – 3328, Oct. 2008.
- [6] R. C. Alferness, “The Evolution of Configurable Wavelength Multiplexed Optical Networks—A Historical Perspective,” *IEEE*, vol. 100, no. 5, pp. 1023–1034, Feb. 2012.
- [7] A. A. M. Saleh and J. M. Simmons, “All-Optical Networking—Evolution, Benefits, Challenges, and Future Vision,” *IEEE*, vol. 100, no. 5, pp. 1105–1117, Mar. 2012.
- [8] D. AMAR, “Performance assessment and modeling of flexible optical networks,” Ph.D. dissertation, Télécom SudParis - Université Pierre et Marie Curie, 2016.
- [9] E. Ip, A. P. T. Lau, D. J. F. Barros, and J. M. Kahn, “Coherent detection in optical fiber systems,” *Optics Express*, vol. 16, no. 2, pp. 753–791, Jan. 2008.

- [10] M. Nakazawa, K. Kikuchi, and T. Miyazaki, Eds. London New York: Springer Heidelberg Dordrecht, 2004.
- [11] I. Chlamtac, A. Ganz, and G. Karmi, “an approach to high bandwidth optical wan’s. Communications,” *IEEE Transactions*, vol. 40, no. 7, pp. 1171–1182, Jul. 1992.
- [12] M. Jinno, H. Takara, B. Kozicki, Y. Tsukishima, T. Yoshimatsu, T. Kobayashi, Y. Miyamoto, K. Yonenaga, A. Takada, O. Ishida, and S. Matsuoka, “Demonstration of novel spectrum-efficient elastic optical path network with per-channel variable capacity of 40 gb/s to over 400 gb/s,” in *Optical Communication, ECOC. 34th European Conference on*, Brussels, Belgium, Sep. 2008, pp. 1–3.
- [13] M. Jinno, “Elastic Optical Networking: Roles and Benefits in Beyond 100-Gb/s Era,” *IEEE Transactions*, vol. 35, no. 5, pp. 1116–1124, Mar. 2017.
- [14] *White paper: Cisco VNI Forecast and Methodology, 2015-2020*, 2016 (accessed December 27, 2016), <http://www.cisco.com/c/en/us/solutions/collateral/service-provider/visual-networking-index-vni/complete-white-paper-c11-481360.html>.
- [15] H. Takara, T. Goh, K. Shibahara, K. Yonenaga, S. Kawai, and M. Jinno, “Experimental demonstration of 400 gb/s multi-flow, multi-rate, multi-reach optical transmitter for efficient elastic spectral routing,” in *Optical Communication, ECOC. 37th European Conference on*, Geneva, Switzerland, Sep. 2011, pp. 1–3.
- [16] F. Buchali, “Technologies towards Terabit Transmission Systems,” in *Optical Communication, ECOC. 36th European Conference on*, Turin, Italy, Sep. 2010, pp. 1–3.
- [17] M. Cantono, A. Ferrara, U. Waheed, A. Ahmad, S. M. H. Zaidi, A. Bianco, and V. Curri, “Networking benefit of hybrid fiber amplification for lightpath regenerators saving,” in *Optical Communication, ECOC. 43rd European Conference on*, Los Angeles, CA, USA, Mar. 2017, pp. 1–3.
- [18] S. T. Naimi, S. P. O. Duill, and L. P. Barry, “Detailed Investigation of the Pump Phase Noise Tolerance for Wavelength Conversion of 16-QAM Signals Using FWM,” *Journal of Optical Communications and Networking*, vol. 6, no. 9, pp. 793–800, Aug. 2014.
- [19] H. N. Tan, T. Inoue, K. Tanizawa, S. Namiki, S. Petit, Y. Oikawa, S. Takasaka, and T. Yagi, “Development of Highly Cascadable Wavelength Converter for All-Optical Networks,” in *The International Conference on Advanced Technologies for Communications (ATC’14)*, 2014, pp. 1–6.
- [20] S. T. Naimi, S. P. O. Duill, and L. P. Barry, “All Optical Wavelength Conversion of Nyquist-WDM Superchannels Using FWM in SOAs,” *Journal of Lightwave Technology*, vol. 33, no. 19, pp. 3959–3967, Oct. 2015.

- [21] H. N. Tan, T. Inoue, K. Solis-Trapala, S. Petit, Y. Oikawa, K. Ota, S. Takasaka, T. Yagi, M. Pelusi, and S. Namiki, "On the Cascadability of All-Optical Wavelength Converter for High-Order QAM Formats," *Journal of Lightwave Technology*, vol. 34, no. 13, pp. 3194–3205, Jul. 2016.
- [22] X. Wang, I. Kim, Q. Zhang, P. Palacharla, and T. Ikeuchi, "Network utilization improvement using format-agnostic multi-channel wavelength converters," in *In Optical Fiber Communications Conference and Exhibition (OFC)*, Anaheim, CA, USA, Mar. 2016, pp. 1–3.
- [23] K. Ishii, T. Inoue, I. Kim, X. Wang, H. N. Tan, Q. Zhang, T. Ikeuchi, and S. Namiki, "Efficient all-optical wavelength converter placement and wavelength assignment in optical networks," in *In Optical Fiber Communications Conference and Exhibition (OFC)*, Anaheim, CA, USA, Mar. 2017, pp. 1–3.
- [24] —, "Analysis and Demonstration of Network Utilization Improvement Through Format-Agnostic Multi-Channel Wavelength Converters," *Journal of Optical Communications and Networking*, vol. 10, no. 2, pp. A165–A174, Feb. 2018.
- [25] Y. B. M'Sallem, A. Shen, F. Lelarge, F. Pommereau, D. Make, S. LaRochelle, and L. A. Rusch, "Quantum-Dash Mode-Locked Lasers for Tunable Wavelength Conversion on a 100 GHz Frequency Grid," *Journal of Optical Communications and Networking*, vol. 4, no. 9, pp. A69–A76, Sep. 2012.
- [26] Y. B. M'Sallem, C. S. Park, S. LaRochelle, and L. A. Rusch, "Multi-Format Wavelength Conversion Using Quantum Dash Mode-Locked Laser Pumps," *Photonics*, vol. 2, no. 2, pp. 527–539, May 2015.
- [27] Y. B. Msallem, "Optical packet networks: enabling innovative switching technologies," Ph.D. dissertation, Université Laval, 2014.
- [28] E. Ciaramella, "Wavelength Conversion and All-Optical Regeneration: Achievements and Open Issues," *Journal of Lightwave Technology*, vol. 30, no. 4, pp. 572–582, Feb. 2012.
- [29] P. N. Tran, "Wdm network planning and management," Ph.D. dissertation, Technical University of Hamburg, 2010.
- [30] H. Zang, J. P. Jue, and B. Mukherjee, "A Review of Routing and Wavelength Assignment Approach for Wavelength routed Optical WDM Networks," *OPTICAL NETWORKS MAGAZINE*, pp. 47 – 59, January 200.
- [31] A. Ahmad, A. Bianco, H. Chouman, G. Marchetto, S. Tahir, and V. Curri, "Exploiting the transmission layer in logical topology design of flexible-grid optical networks," in *IEEE International Conference on Communications (ICC)*, Kuala Lumpur, Malaysia, May. 2016, pp. 1–6.

- [32] H. Chouman, M. Lourdiane, and C. Ware, "Impact of traffic serving order on mixed-line-rate Optical Network performances," in *19th International Conference on Transparent Optical Networks (ICTON)*, Girona, Spain, Jul. 2017, pp. 1–3.
- [33] J. P. Jue, "Lightpath establishment in wavelength-routed wdm optical networks," in *Optical Networks. Network Theory and Applications*, R. L. and D. DZ., Eds. Boston, MA: Springer, Boston, MA, 2001, pp. 99–122.
- [34] E. W. Dijkstra, "A Note on Two Problems in Connexion with Graphs," *Numerische Mathematik*, vol. 1, no. 1, pp. 269 – 271, June 1959.
- [35] N. Sambo, M. Secondini, F. Cugini, G. Bottari, P. I. F. Cavaliere, and P. Castoldi, "Modeling and distributed provisioning in 10-40-100-gb/s multirate wavelength switched optical networks," *Journal of Lightwave Technology*, vol. 29, no. 9, pp. 1248 – 1257, May. 2011.
- [36] T. Inoue, K. Tanizawa, and S. Namiki, "Guard-Band-Less and Polarization-Insensitive Tunable Wavelength Converter for Phase-Modulated Signals: Demonstration and Signal Quality Analyses," *Journal of Lightwave Technology*, vol. 13, no. 10, pp. 1981–1990, May 2014.
- [37] F. Buchali, L. Schmalen, Q. Hu, and D. Che, "Low latency digital regenerator for dual polarization QAM signals," in *European Conference on Optical Communication (ECOC)*, Sep. 2015.
- [38] M. Kovacevic and A. Acampora, "Benefits of wavelength translation in all-optical clear-channel networks," *IEEE Journal on Selected Areas in Communications*, vol. 14, no. 5, pp. 868–880, June 1996.
- [39] R. Barry and P. Humblet, "Models of Blocking Probability in All-Optical Networks with and without Wavelength Changers," *IEEE Journal on Selected Areas in Communications*, vol. 14, no. 5, pp. 858–867, June 1996.
- [40] S. Subramaniam, M. Azizoglu, and A. Somani, "All-optical networks with sparse wavelength conversion," *IEEE/ACM Transactions on Networking*, vol. 4, no. 4, pp. 544 – 557, Aug. 1996.
- [41] A. Mokhtar and M. Azizoglu, "Adaptive Wavelength Routing in All-Optical Networks," *IEEE/ACM Transactions on Networking*, vol. 6, no. 2, pp. 197 – 206, April 1998.
- [42] E. Karasan and E. Ayanoglu, "Effects of Wavelength Routing and Selection Algorithms on Wavelength Conversion Gain in WDM Optical Networks," *IEEE/ACM Transactions on Networking*, vol. 6, no. 2, pp. 186 – 196, April 1998.
- [43] S. Ramamurthy and B. Mukherjee, "Fixed-Alternate Routing and Wavelength Conversion in Wavelength-Routed Optical Networks," in *IEEE GLOBECOM*, Nov. 1998, pp. 2295 – 2302.

- [44] B. Li and X. Chu, "Routing and Wavelength Assignment vs. Wavelength Converter Placement in All-Optical Networks," *IEEE Communications Magazine*, vol. 41, no. 8, pp. S22 – S28, Aug. 2003.
- [45] B. Li, X. Chu, and I. Chlamtac, "Wavelength Converter Placement Under Different RWA Algorithms in Wavelength-Routed All-Optical Networks," *IEEE Transaction on Communications*, vol. 51, no. 4, pp. 607 – 617, Apr. 2003.
- [46] B. Li and X. Chu, "Dynamic Routing and Wavelength Assignment in the Presence of Wavelength Conversion for All-Optical Networks," *IEEE Transactions on Networking*, vol. 13, no. 3, pp. 704 – 715, Jun. 2005.
- [47] K. Christodoulopoulos, K. Manousakis, and E. Varvarigos, "Adapting the transmission reach in mixed line rates wdm transport networks," in *The 15th International Conference on Optical Networking Design and Modeling (ONDM)*, Feb. 2011.
- [48] C. S. K. Vadrevu, R. Wang, M. Tornatore, C. U.Martel, and B. Mukherjee, "Degraded service provisioning in mixed-line-rate wdm backbone networks using multipath routing," *Journal of Lightwave Technology*, vol. 22, no. 3, pp. 840 – 849, 2014.
- [49] H. Cukurtepea, A. Yayimlia, and B. Mukherjeeb, "Impairment-aware lightpath provisioning using inverse multiplexing in mixed-line-rate networks," *Optical Switching and Networking*, vol. 11, pp. 44 – 52, Jan. 2014.
- [50] G. B. Algin and E. T. Tunali, "Cost efficient line rate assignment strategy wdm optical networks," in *The 19th International Conference on Optical Networking Design and Modeling (ONDM)*, Feb. 2015.
- [51] S. Iyer, "A survey on next-generation mixed line rate (mlr) and energy-driven wavelength-division multiplexed (wdm) optical networks," *Journal of Optical Communications and Networking*, vol. 36, no. 2, pp. 137 – 153, 2015.
- [52] P. Poggiolini, G. Bosco, A. Carena, V. Curri, Y. Jiang, and F. Forghieri, "The gn-model of fiber non-linear propagation and its applications," *Journal of Lightwave Technol.*, vol. 32, no. 4, pp. 694–721, feb 2014.
- [53] P. Poggiolini, "The gn model of non-linear propagation in uncompensated coherent optical systems," *J. Lightwave Technol.*, vol. 30, no. 24, pp. 3857–3879, Dec. 2012.
- [54] M. N. Chughtai, "Study of physical layer impairments in high speed optical networks," Master's thesis, KTH School of Information and Communication Technology, Stockholm, Sweden, 2012.
- [55] G. P. Agrawal, Ed. Elsevier, 2008.
- [56] S. P. Singh and N. Singh, "Nonlinear effects in optical fibers: Origin, management and applications," *Progress In Electromagnetics Research*, vol. 73, pp. 249 – 275, 2007.

- [57] A. Bononi, M. Bertolini, P. Serena, and G. Bellotti, “Error probability of dpsk signals with cross-phase modulation induced nonlinear phase noise,” *JOURNAL OF LIGHTWAVE TECHNOLOGY*, vol. 27, no. 18, pp. 3974 – 3983, SEP. 2009.
- [58] J.-P. Faure, B. Lavigne, C. Besson, O. Bertran-Pardo, A. C. Colomer, and R. Canto, “40g and 100g deployment on 10g infrastructure: market overview and trends, coherent versus conventional technology,” in *Optical Fiber Communication (OFC) conference*, Mar. 2019.
- [59] *Spectral grids for WDM applications: CWDM wavelength grid, ITU-T G.694.1.*
- [60] A. Nag, M. Tornatore, and B. Mukherjee, “Energy-efficient and cost-efficient capacity upgrade in mixed-line-rate optical networks,” *Journal of Optical Communications and Networking*, vol. 4, no. 9, pp. 1018 – 1025, Dec. 2012.
- [61] D. Penninckx and C. Perret, “New physical analysis of 10-gb/s transparent optical networks,” *Photonics Technology Letters*, vol. 15, no. 5, pp. 778 – 780, May 2003.
- [62] J. P. Gordon and L. F. Mollenauer, “Phase noise in photonic communications systems using linear amplifiers,” *Optical Letters*, vol. 15, no. 23, pp. 1351 – 1353, Apr. 1990.
- [63] K.-P. Ho, “Error probability of dpsk signals with cross-phase modulation induced nonlinear phase noise,” *IEEE JOURNAL OF SELECTED TOPICS IN QUANTUM ELECTRONICS*, vol. 10, no. 2, pp. 421 – 427, Apr. 2014.
- [64] P. Poggiolini, G. Bosco, A. Carena, V. Curri, Y. Jiang, and F. Forghieri, “The gn model of fiber non-linear propagation and its application,” *J. Lightwave Technol.*, vol. 32, no. 4, pp. 694–721, February 2012.
- [65] A. Carena, G. Bosco, V. Curri, P. Poggiolini, M. T. Taiba, and F. Forghieri, “Statistical characterization of PM-QPSK signals after propagation in uncompensated optical links,” in *36th European Conference and Exhibition on Optical Communication (ECOC)*, Torino, Italy, Sep. 2010, pp. 4–7.
- [66] A. Nucci, A. Sridharan, and N. Taft, “The problem of synthetically generating ip traffic matrices: Initial recommendations,” *ACM SIGCOMM Computer Communication*, vol. 35, no. 2, pp. 19 – 32, . 2005.
- [67] A. Eira, J. Pedro, , and J. Pires, “ On the impact of optimized guard-band assignment for superchannels in flexible grid optical networks,” in *Optical Fiber Communication Conference and Exposition and the National Fiber Optic Engineers Conference (OFC/NFOEC)*, March 2013, pp. 4–7.
- [68] “The open-source network planner: Net2plan,” <http://www.net2plan.com/>.

Titre: Conception et évaluation des performances des réseaux à conversion de longueur d'onde tout-optique gérant les dégradations du signal

Mots clés: Réseaux Optique, conversion de longueur d'onde tout-optique, routage et assignation de longueur d'onde, heuristiques, MLR, dégradation de la transmission par fibre

Résumé: La croissance continue du trafic Internet implique une augmentation de la consommation d'énergie en raison des nombreuses conversions optique à électronique (OEO) requises par les routeurs et les commutateurs. L'utilisation de réseaux transparents pourraient freiner cette croissance incontrôlée, mais le maintien des données dans le domaine optique a deux conséquences néfastes: une accumulation du bruit et des non-linéarités de l'amplification qui dégrade fortement les performances au niveau de la couche physique. et la contrainte de continuité de longueur d'onde (WCC) reflétant la conservation de la longueur d'onde du signal optique dans les réseaux optiques multiplexés en longueur d'onde (WDM) qui dégradent les performances du réseau, notamment sa probabilité de blocage. Les convertisseurs de longueur d'onde (WC) peuvent pallier la contrainte WCC, mais les seuls dispositifs suffisamment matures disponibles dans le commerce sont les WC basés sur OEO (OEO-WC). Cependant, leur coût augmente avec les débits binaires. D'autre part, des convertisseurs de longueur

d'onde tout optique (AO-WC) ont été démontrés dans des laboratoires de recherche, avec toutefois une plage de conversion limitée et une dégradation du signal converti.

Dans cette thèse, nous concevons la couche de transmission en utilisant deux ensembles de formats de modulation différents avec des plages de débits différentes; et par conséquent différents modèles d'estimation de performance. Au niveau du réseau, nos analyses montrent que la contribution des WC dépend des demandes de trafic servant à l'ordre dans un scénario de planification du réseau; qu'en utilisant des algorithmes fixed-alternate-routing (FAR) ou least-loaded-routing (LLR) et un algorithme d'affectation de longueur d'onde first-fit (FF), les AO-WCs offrent les mêmes améliorations de performances que les OEO-WC. De plus, nous identifions une plage de conversion et une cascabilité optimale d'AO-WC qui montre que le LLR nécessite un nombre de conversions par canal inférieur au FAR.

Title: Impairment-aware design and performance evaluation of all-optical wavelength convertible networks

Keywords: Optical Networks, RWA, All-optical wavelength converters, Mixed-line-rate, Fiber Transmission Impairments

Abstract: The continuous growth of Internet traffic implies an increased power consumption due to the many optical-to-electronic (OEO) conversions required by routers and switches. Transparent networks could curb this uncontrolled growth, but keeping the data in the optical domain has two adverse consequences: physical layer impairments accumulation which strongly degrades the performance due to amplification noise and non-linearities; and the wavelength continuity constraint (WCC) to keep the optical signal's wavelength unchanged in wavelength-division-multiplexed (WDM) optical networks which degrades network blocking performance. Wavelength converters (WCs) can alleviate the WCC constraint, but the only commercially available devices are the OEO-based WCs (OEO-WCs), however, their cost increases with bit-rates. On the other hand, all-optical wavelength converters (AO-WCs) have been demonstrated in re-

search laboratories albeit with a limited conversion range and a performance that degrades converted signal's quality.

In this thesis, we design the transmission layer using two different modulation formats sets with different bit-rates ranges; and consequently different performance estimation models. At the network level, our analyses show that WCs' contribution depends on traffic demands serving ordering in the offline traffic assumption; that using fixed-alternate routing (FAR) or least-loaded routing (LLR) algorithms and first-fit (FF) wavelength assignment algorithm, AO-WCs give the same performance enhancement as OEO-WCs. Moreover, we identify an optimum AO-WC conversion range and cascability which shows that LLR requires lower number of conversions per channel compared to FAR.

Université Paris-Saclay
Espace Technologique / Immeuble Discovery
Route de l'Orme aux Merisiers RD 128 / 91190 Saint-Aubin, France

